

FG-431621N

RSC-3622-2

"Made available under NASA sponsorship
in the interest of early and wide dis-

semination of (E80-10063) CORRELATION OF SPACECRAFT
Program for us PASSIVE MICROWAVE SYSTEM DATA WITH SOIL
MOISTURE INDICES (API) - Progress Report,
Feb. - Aug. 1979 (Texas A&M Univ.), 66 p
HC A04/MF A01

N80-18513

Unclassified
CSCL 08M G3/43 00063

80-10063
CR-162585

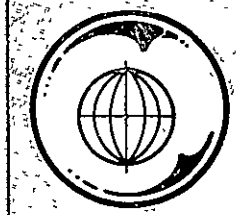
CORRELATION OF SPACECRAFT PASSIVE MICROWAVE SYSTEM DATA WITH SOIL MOISTURE INDICES (API)

By

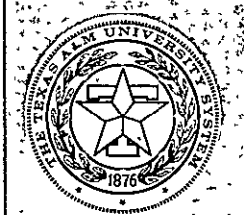
Bruce J. Blanchard
Remote Sensing Center
Texas A&M University
College Station, Texas 77843

Progress Report for Period
February 1979 - August 1979

Prepared for
Goddard Space Flight Center
Greenbelt, Maryland 20771
Contract No.: NSG-5193



TEXAS A&M UNIVERSITY
REMOTE SENSING CENTER
COLLEGE STATION, TEXAS



CORRELATION OF SPACECRAFT PASSIVE MICROWAVE
SYSTEM DATA WITH SOIL MOISTURE INDICES (API)

By

Bruce J. Blanchard
Remote Sensing Center
Texas A&M University
College Station, Texas 77843

Progress Report for Period
February 1979 - August 1979

Prepared for
Goddard Space Flight Center
Greenbelt, Maryland 20771

Contract No.: NSG-5193

TABLE OF CONTENTS

	Page
LIST OF FIGURES	ii
1.0 INTRODUCTION	1
2.0 BACKGROUND	2
3.0 PROJECT DESCRIPTION.	4
4.0 PRESENT STATUS OF CONTRACT REQUIREMENTS.	8
4.1 Procedure	8
4.2 The Soil Moisture Model	8
4.3 Emissivity Model.	10
4.4 Analysis and Discussion	11
5.0 CONCLUSION	22
6.0 LITERATURE CITED	24
APPENDIX A.	26
APPENDIX B.	60

LIST OF FIGURES

Figure	Page
1 Southern Great Plains Area To Be Used As A Basis for Calibration of ESMR	5
2 Gridded Area Used By McFarland in Pre- liminary Study and As Training Site Grid . . .	6
3 Percentages of Area Devoted to Winter Wheat and Total Croplands by County. The First Number Is Percent Winter Wheat. The Second Is Percent Croplands Including Winter Wheat	13
4 Fall (August 12-November 1) correlation Coefficients for Each Grid Point (Values are Multiplied by -100)	14
5 Spring (February 28-April 15) Correlation Coefficients for Each Grid Point	16
6 Fall Scatter Plot for Six Winter Wheat Grid Points	17
7 Fall Scatter Plot for Six Non-Wheat Croplands Grid Points.	18
8 Spring Scatter Plot for Six Winter Wheat Grid Points.	20
9 Spring Scatter Plot for Six Non-Wheat Croplands Grid Points.	21

1.0 INTRODUCTION

Estimates of surface soil moisture in a large area context are primarily useful for large area crop monitoring, estimating flood hazards, and as inputs into dynamic atmospheric models. Such estimates may also provide indications of soil moisture below the surface as well as provide a means for the determination of drought and aerial extent of drought conditions. Conventional soil moisture measurement are very time consuming and not widely or regularly obtained over most of the United States. The spatial variation of soil moisture make it difficult to extrapolate conventional point measurements to represent an integrated value over a large area. Two alternative techniques for obtaining large area estimates of soil moisture are water balance and remote sensing methods.

The attention of this study is focused on the latter and is specifically directed toward testing and improving correlations between passive microwave antenna temperatures from space and indices of soil moisture over a large area in the southern Great Plains. The two microwave systems to be used are the Electrically Scanning Microwave Radiometer (ESMR) and the Scanning Multichannel Microwave Radiometer (SMMR). This progress report will only consider the ESMR because SMMR data is not presently available.

2.0 BACKGROUND

The 1.55 cm. ESMR is a quasi-operational spacecraft system from which digital data can be acquired over the same area on approximately a 3-day repeat cycle. This affords the opportunity to use time series data for multi-temporal mapping. Recent investigations by Cihlar and Ulaby (1975), Meneely (1977), Schmugge et al. (1974, 1976a and 1976b), Schmugge (1976 and 1977) and Newton (1977) have demonstrated that surface emissivity at the 1.55 cm. wavelength is inversely related to soil moisture content in the surface layer. Sensitivity of this emissivity to moisture content is significantly diminished by an increase in surface roughness, and/or an increase in vegetation density. Consequently, the most significant results have been obtained on relatively bare, smooth soils.

Schmugge et al. (1977) presented case studies of ESMR's spatial response to recent rainfall as related to vegetation and surface roughness. Relative vegetation densities was obtained from Landsat false color infrared images and surface roughness features were inferred from U.S. Geological Survey surface land forms. Their results show that variations in surface roughness and vegetative cover plus the absence of large areas of bare soils restrict the spatial mapping capabilities of soil moisture at satellite altitudes.

Temporal mapping of soil moisture shows a greater potential than other methods because the adverse effects of point-to-point variations of surface roughness and vegetation cover are minimized (McFarland and Blanchard, 1977). The moisture content and temperature of the emitting layer integrated over the sensor footprint forms the major variations of temporal brightness temperature changes. Since the emitting layer temperature can be approximated, the brightness temperature changes may provide a fairly accurate indication of soil moisture changes from rainfall and subsequent drying. By using temporal mapping techniques with ESMR, McFarland and Blanchard obtained high correlations between microwave emissivity and soil moisture modeled by antecedent precipitation indices (API) during the autumn (minimum vegetative period) over relatively flat terrain.

3.0 PROJECT DESCRIPTION

A large region of the southern Great Plains is being used as a basis for calibration of passive microwave systems as an estimator of antecedent precipitation which in turn is related to soil moisture (Figure 1). This region was selected for two reasons: first, it encompasses the area used by McFarland and Blanchard (1977) in the preliminary study of ESMR data, and, secondly, the area is a principle source of hard winter wheat. This study will expand McFarland and Blanchard's temporal techniques to include vegetated seasons over a span of several years.

Daily values of precipitation and air temperatures and all available ESMR brightness temperatures over this region will be related to a 25 x 25 km grid. These values will then be used to model emissivity and API in such a way as to optimize their correlation. The block of grid points used by McFarland and shown in Figure 2 will be used to establish a relationship between effective microwave emissivity and API. The relationship will then be used to predict ESMR antenna temperatures for another large wheat producing area in Kansas using API as an input. Comparison of predicted and actual antenna temperatures in such a relatively independent area should provide verification of the techniques. Simultaneously time series estimation of API values on independent cells will be studied to determine if it is feasible

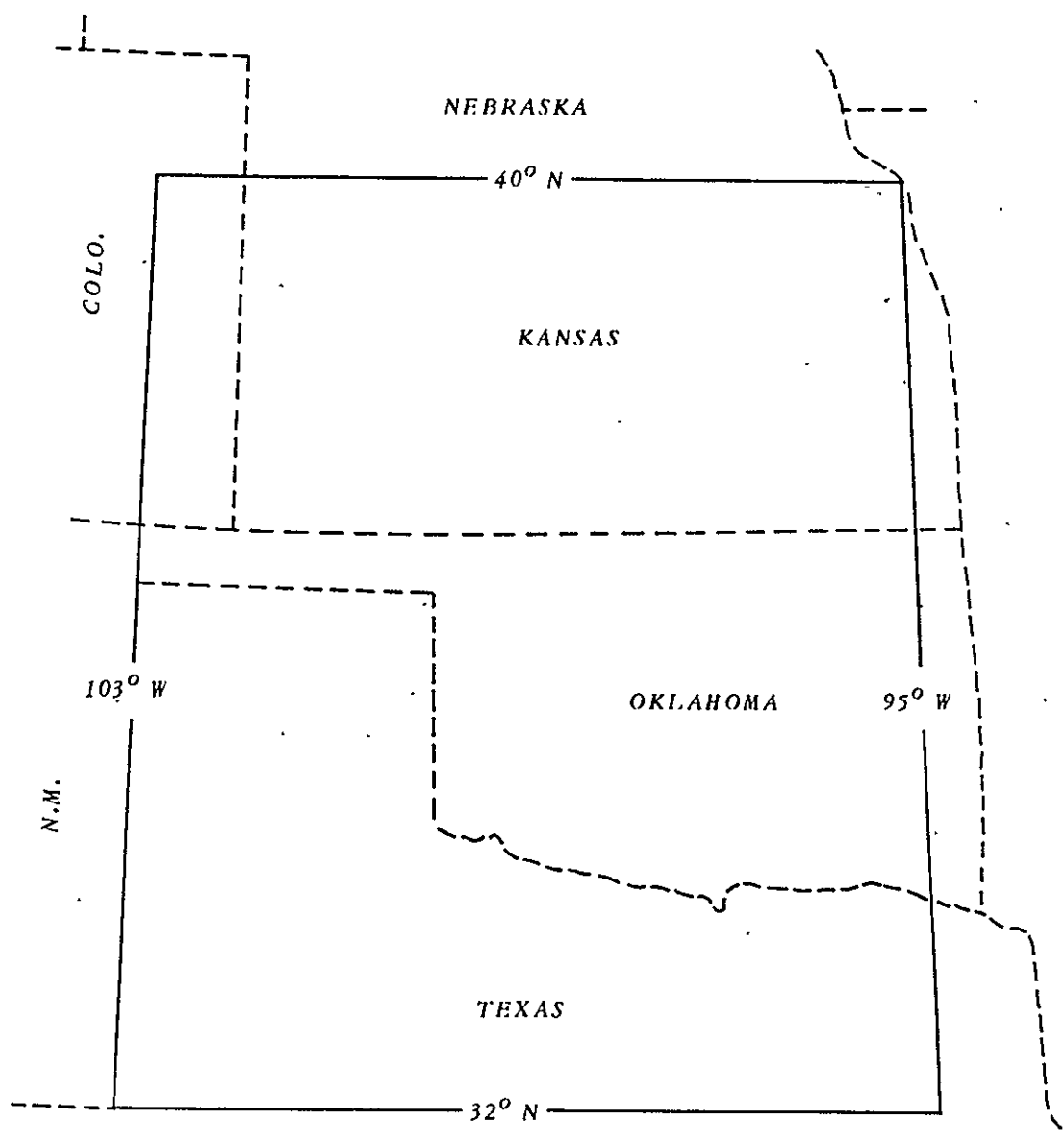


FIGURE 1: Southern Great Plains Area To Be Used
As A Basis For Calibration Of ESMR

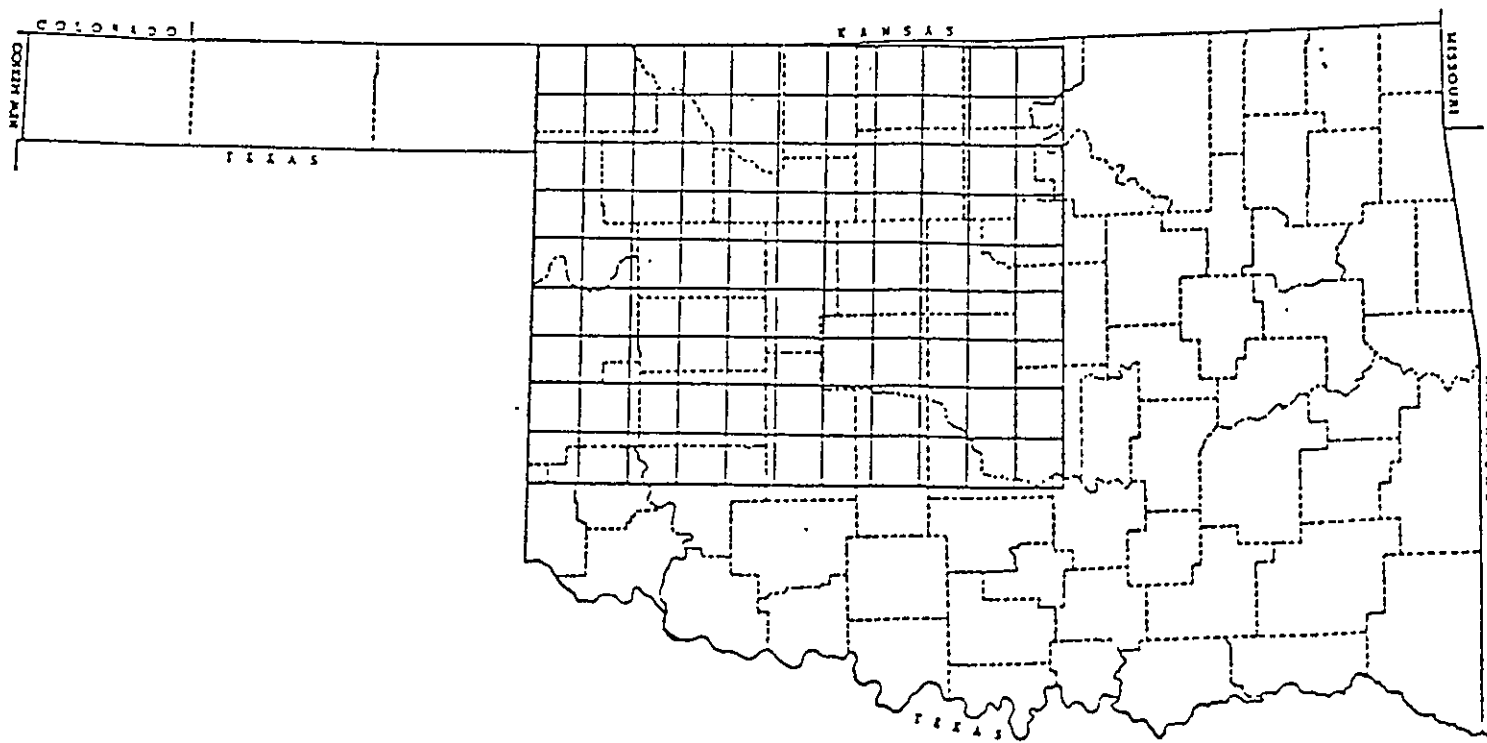


FIGURE 2: Gridded Area Used By McFarland In Preliminary Study and as training site grid.

to use ESMR data to monitor drought conditions in the southern Great Plains.

4.0 PRESENT STATUS OF CONTRACT REQUIREMENTS

4.1 Procedure

ESMR antenna temperatures with appropriate locations for each datum point have been received for the southern Great Plains. The time frame of this data is September 1973 through May 1975 with a large gap in the data during the summer of 1974. Daily precipitation and temperature data tapes have been received for the region for 1973 through 1976. These data and the ESMR data have been resampled to emulate two separate grids with 25 km cells based on polar stereographic projections. The training site grid is the same as McFarland and Blanchard's (Figure 2) with projection true at 35° latitude. The other grid extends over the entire study area (Figure 1) and has its projection true at 37° latitude. The grid point values were objectively analyzed by using a modified Barnes exponential technique (Barnes, 1973). The spatially grid data was then realigned temporally in order to prepare each grid point for multi-temporal analysis.

4.2 The Soil Moisture Model

In the absence of actual soil moisture measurements, a simple soil moisture model was used to account for changes in moisture in the ESMR emitting layer. An antecedent precipitation index (API) was selected because of its simplicity

and its ability to infer upper-level soil moisture. The only input required by API is precipitation which, for large areas, is readily available from climatological data. Effective precipitation was considered a direct input to the soil water storage that is estimated by the API. Losses of soil moisture due to evaporation and transpiration were assumed to decrease exponentially with time (Linsley, Kohler and Paulhus, 1975). Shown mathematically, the relationship is

$$API_i = P_i k^t \quad (1)$$

where P is effective precipitation, i is the day number, t is the time after rainfall, and k is a recession factor which accounts for seasonal differences in evapotranspiration losses.

Rather than total the combined influence of all the rainfall events in a period, daily indexes were calculated by setting t equal to 1. This yielded

$$API_i = P_i + (API_{i-1} \times k) \quad (2)$$

from Equation 1 (Saxton and Lenz, 1967).

Before the first API value was used in a correlation with emissivity, the API model was allowed to stabilize by using a minimum of 30 days of rainfall history. The relationship between rainfall amount (R) and effective precipitation,

developed by Blanchard *et al.* (1979) (included in Appendix A), was used to account for runoff. An empirical recession curve developed at the SEA/AR (Southern Great Plains Watershed Research Center, Chickasha, Oklahoma) by DeCoursey (1974) was used for calculating the daily recession factor k . The final form of the soil moisture model was

$$API_i = R_i^{.891} + (API_{i-1} \times k_i) \quad (3)$$

where

R_i = daily rainfall amount (cm.).

4.3 Emissivity Model

The temperature of the emitting layer was approximated by the daily maximum temperature (T_{MT}) in the emissivity model,

$$\epsilon = T_{BT}/T_{MT} \quad (4)$$

where T_{BT} is the ESMR brightness temperature and ϵ is the emissivity. The emitting layer for the short wavelength ESMR is limited to the top few centimeters. The overpass time of ESMR over the study area is near local noon and maximum air temperature usually occurs several hours later. Because the maximum soil temperature usually leads the maximum air temperature, this is believed to be a sound approximation. The sensitivity of this model to errors in the

emitting layer temperature is small. An error of 10 K will only yield a 4 percent error in the predicted emissivity.

The dielectric properties of ice are completely different than water. Ice is not a dipole molecule and has a low dielectric constant. When a soil is frozen the emissivity is high and independent of soil moisture. Emissivity values were not used in this study if the maximum air temperature was less than 283 K.

Paris (1971) showed that rain in an atmosphere can have a very significant effect on upwelling radiation. Radar summary charts from the NWS were used in determining the presence of rain between ESMR and each surface grid point. When this occurred, the emissivity data points were omitted.

4.4 Analysis and Discussion

During the period of this progress report the study was directed toward developing relationships between emissivity and API over the training grid area in Oklahoma (Figure 2). The results were presented in a thesis by Theis (1979) and by a paper presented at the 1979 AGU Spring Meeting (abstract in Appendix B). These results are summarized and presented here.

The calendar year was divided into four new-standard ESMR seasons because of climatological factors, crop phenologies and cultivation practices. Percentages of areas devoted

to winter wheat and total croplands for the grid area are presented in Figure 3. Fall was defined from August 12 to November 1 which corresponded to a minimum vegetation period when fields are relatively flat. This is the period studied by McFarland and Blanchard (1977) and their results were duplicated. The fall correlation coefficients between emissivity and API for each grid point are presented in Figure 4. By comparing the areas of greater than 0.80 to Figure 3 and Landsat color composites (not presented) it is apparent that cultivated agricultural lands give the best correlations.

Winter, as defined by this study (November 2-February 27), is characterized by periods of frozen soil surfaces and upward movement of moisture due to temperature gradients. The correlations during this period are much less significant with values generally around -0.60. Both the emissivity and API models are not well suited for the winter. The API model is very simple and doesn't account for movement of water due to temperature gradients. The dielectric properties of ice is significantly different than water, making the emissivity independent of soil moisture in the frozen state.

Spring (February 28-April 15) was defined as a rather short season generally bounded by the end of frozen soil surfaces and the beginning of winter wheats boot stage. This is a period of smooth soil surface with increasing vegetative

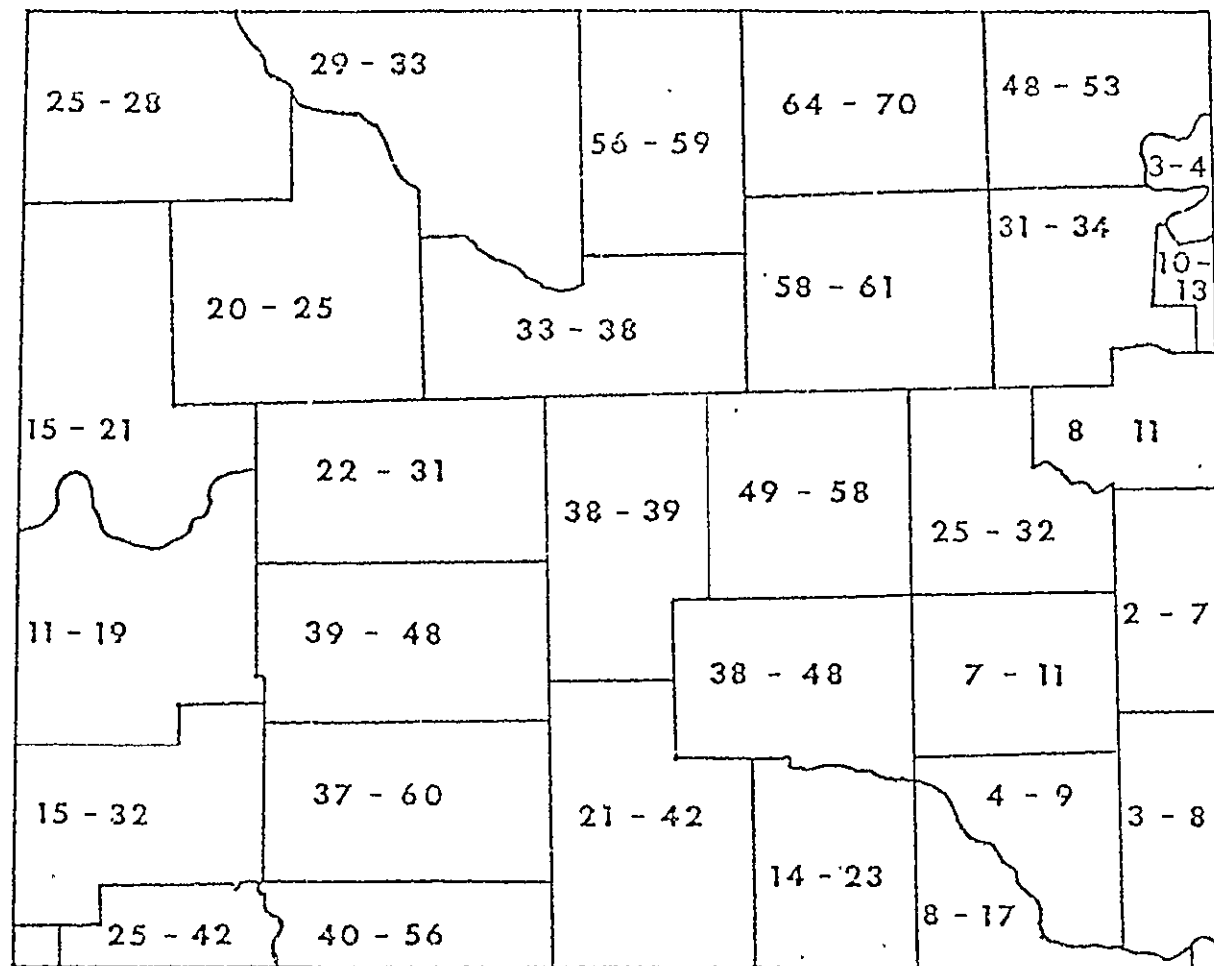


Figure 3. Percentages of area devoted to winter wheat and total croplands by county. The first number is percent winter wheat. The second is percent croplands including winter wheat.

	1	2	3	4	5	6	7	8	9	10	11	12
1	70	76	64	75	82	85	86	82	82	81	68	54
2	69	72	65	75	84	81	88	80	73	82	59	35
3	64	66	66	79	80	80	80	81	78	70	52	41
4	72	73	60	67	71	69	77	76	71	62	55	31
5	64	47	49	72	72	79	80	75	71	64	45	38
6	57	59	67	70	73	80	65	71	63	58	48	48
7	66	72	74	88	84	80	82	73	47	36	52	53
8	65	72	76	89	82	73	71	69	55	40	54	51
9	70	79	85	82	80	66	54	56	53	58	51	56
10	71	85	86	82	76	63	60	57	58	61	41	32

Figure 4. Fall (August 12-November 1) correlation coefficients for each grid point (values are multiplied by -100).

cover over winter wheat acreage. Over other agricultural croplands the soil surface is bare but is either in a rough bedded condition or freshly planted in rows. The good correlation areas, shown in Figure 5, generally correspond with predominantly winter wheat agricultural areas. This shows up quite well when the grid is overlayed onto a Landsat color composite taken during April when the only growing vegetation is winter wheat.

All croplands are densely vegetated during summer (April 16-June 8) as defined in this study. Correlation coefficients are corresponding poorly with values averaging around -0.50.

The differences between the spring correlations of winter wheat and non-wheat croplands were investigated further by plotting six grid points from each area. The plots for fall, shown in Figures 6 and 7, indicate very little differences in the two areas. The values of the slopes and intercepts agree closely with those obtained by McFarland and Blanchard (1977) (slope = -0.0232, intercept = 0.92). It should be pointed out that McFarland used one year's data and this study used two.

Spring scatter plots are presented in Figures 8 and 9. Correlations for the winter wheat area are significantly higher than non-wheat croplands. The slope for the winter wheat areas has slightly decreased from the fall value

	1	2	3	4	5	6	7	8	9	10	11	12
1	72	76	69	68	60	78	80	72	74	78	56	44
2	67	70	75	79	81	79	71	76	78	81	45	32
3	71	72	78	80	77	81	76	72	77	72	53	39
4	68	34	57	75	75	79	78	72	72	62	32	46
5	50	61	69	73	72	73	69	69	58	61	65	70
6	39	57	65	63	70	70	72	71	79	61	64	59
7	57	56	64	81	75	68	62	76	65	55	63	64
8	66	63	63	71	64	54	65	68	59	54	71	71
9	57	69	69	62	58	57	65	54	58	66	73	79
10	58	66	50	49	43	58	64	62	69	68	79	75

Figure 5. Spring (February 28-April 15) correlation coefficients for each grid point (values are multiplied by -100).

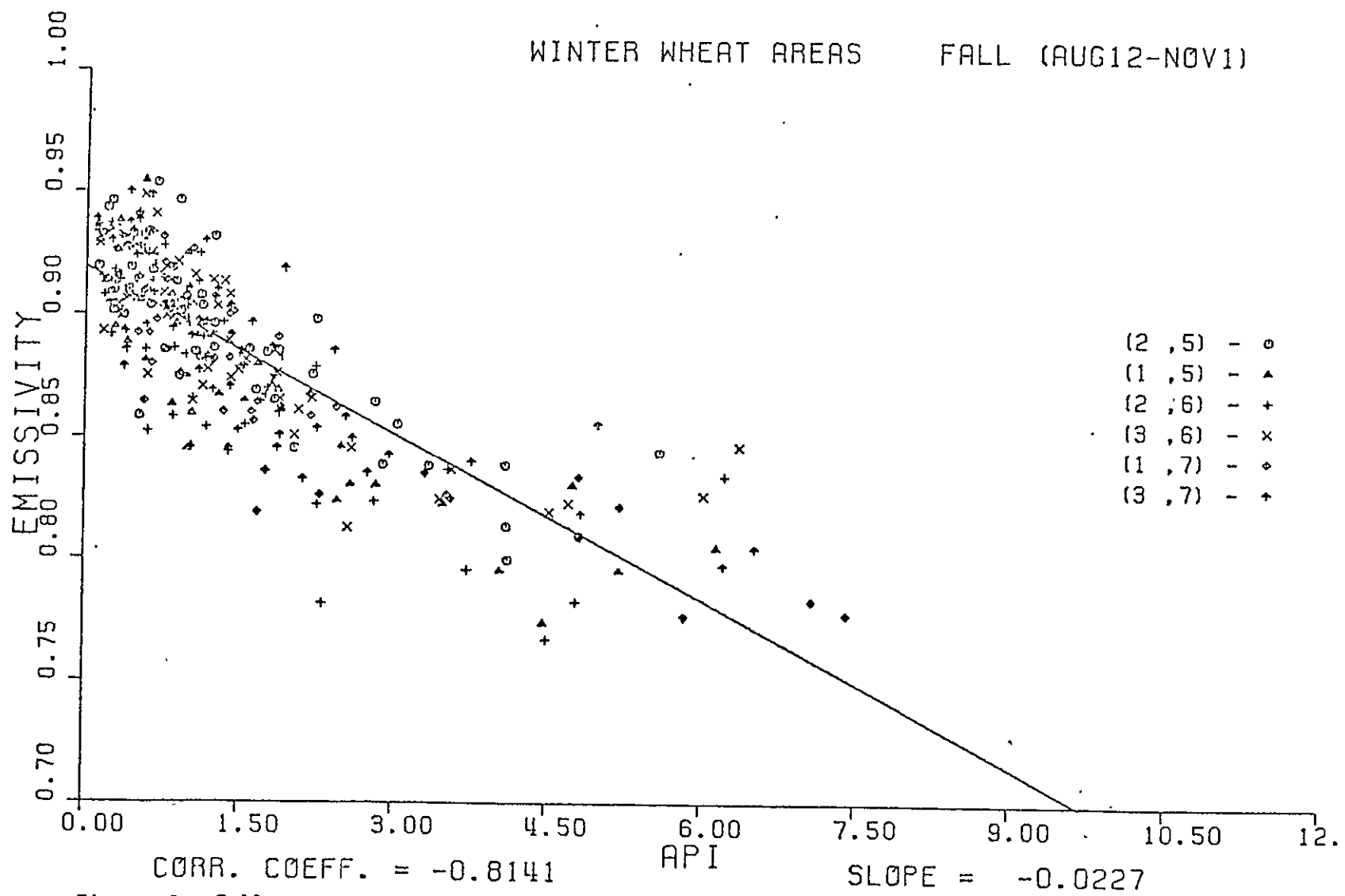


Figure 6. Fall scatter plot for six winter wheat grid points.

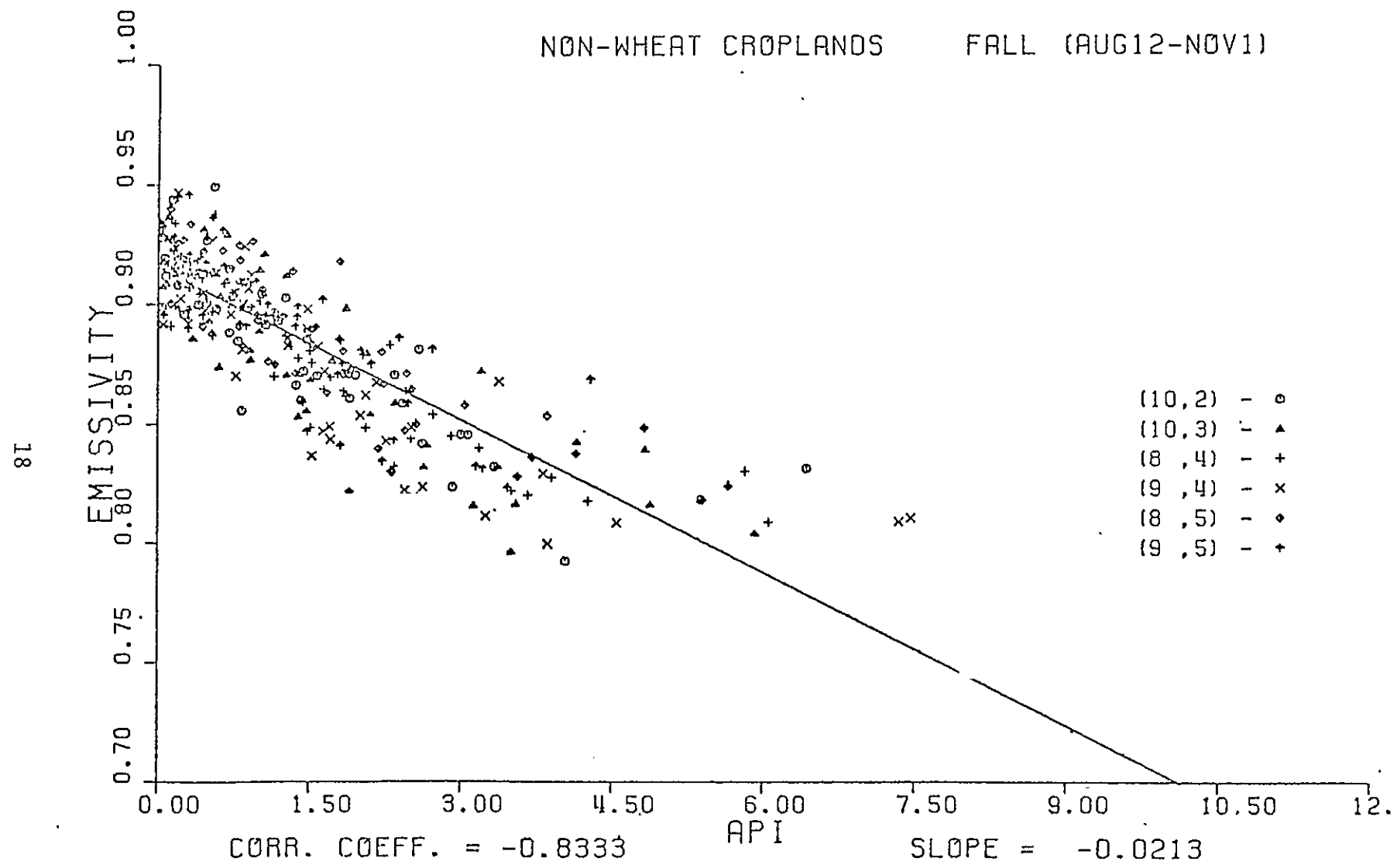


Figure 7. Fall scatter plot for six non-wheat croplands grid points.

(-0.0227 to -0.0156). This indicates that the small winter wheat vegetation may affect but doesn't destroy the good relationship. The summer slope for the same grid points decreases to -0.0081 with a corresponding correlation coefficient of -0.48. During summer the vegetation has reached a threshhold density so that ESMR's response to API becomes masked by the vegetation.

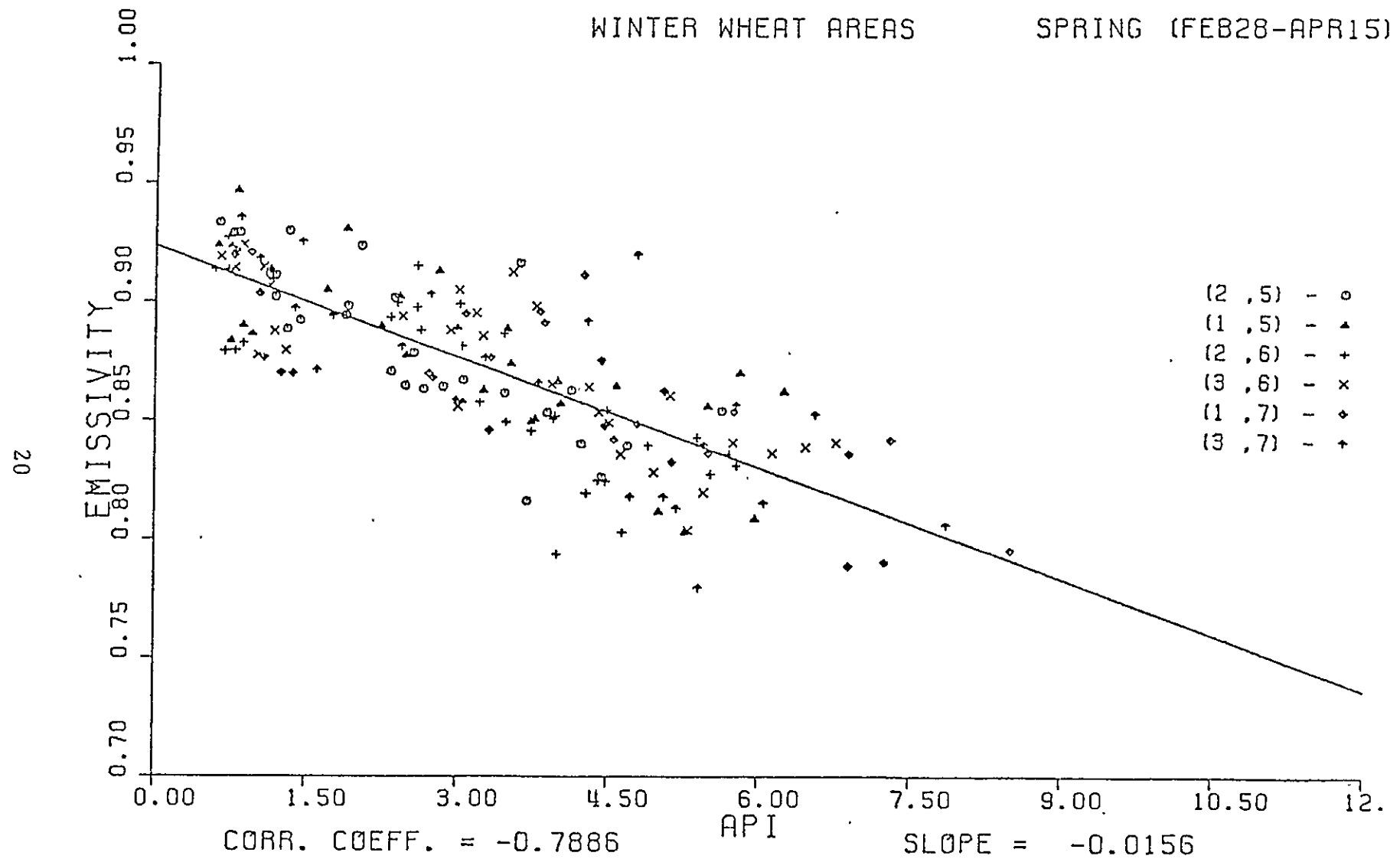


Figure 8. Spring scatter plot for six winter wheat grid points.

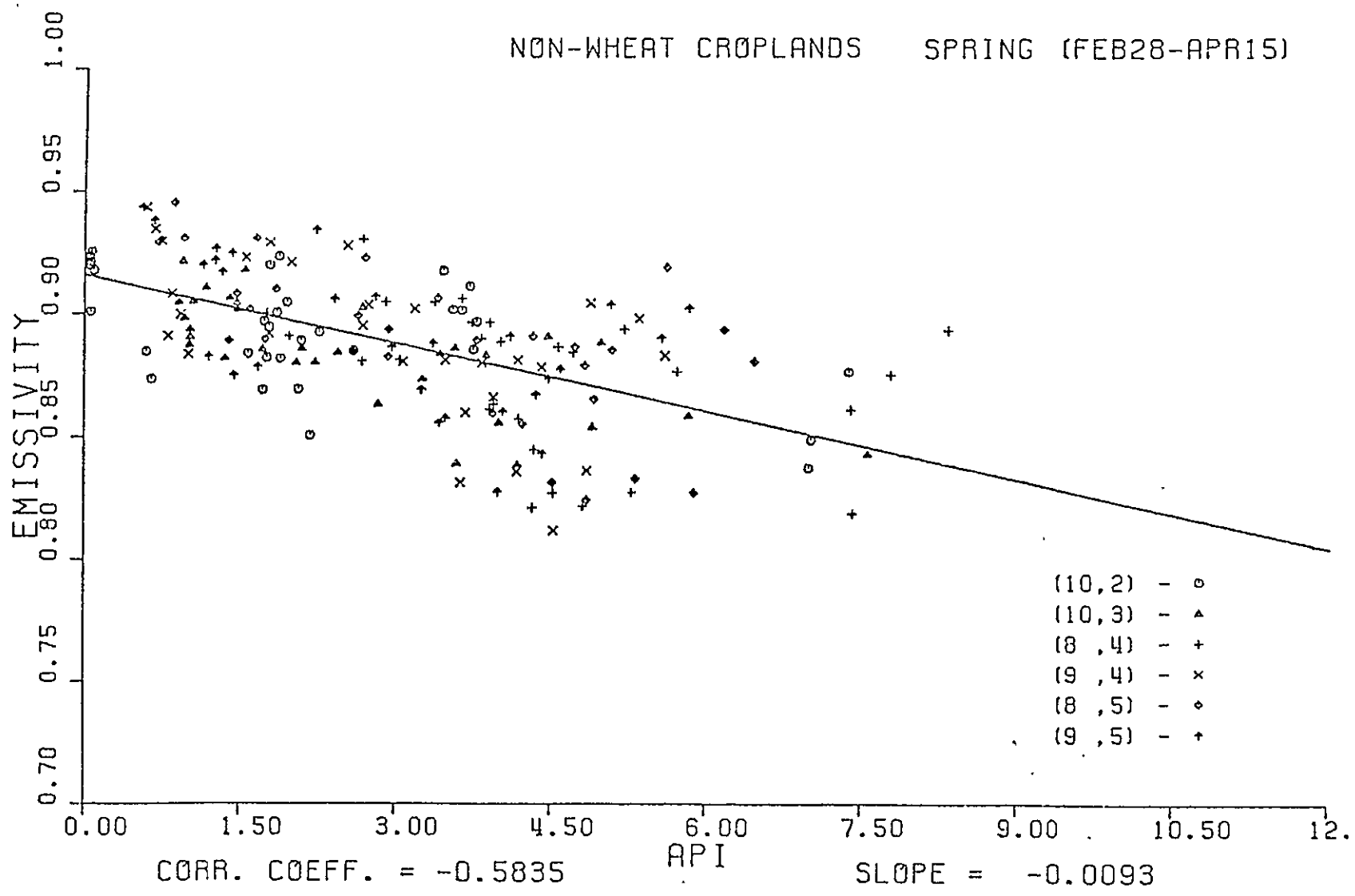


Figure 9. Spring scatter plot for six non-wheat croplands grid points.

5.0 CONCLUSION

Agricultural lands show the greatest potential to use ESMR to infer soil moisture. These usually are better soils situated on smoother, less hilly, land. Tillage practices are such as to afford periods of smooth and bare soils during the year. In contrast, pastures, rangelands and cross timber usually are situated on poorer soils (some rocky) and terrain which is unsuitable for agriculture. The surface of untilled lands is almost never completely bare. It is covered with growing or dead vegetation or with timber.

Winter wheat yields are more sensitive to water stress at some growth stages than others. There must be sufficient moisture in fall in order to sprout the winter wheat and sustain it until winter. During winter, soil moisture usually is sufficient for the crop's needs.

Soil moisture during spring is very important in the determination of wheat yield. The wheat begins jointing in March and enters the boot stage in mid-April. The weeks before booting are the most critical period because this is when the crop is set. After the boot stage, ample soil moisture is preferred to reduce shrinkage but is not as critical.

Results over the predominant winter wheat areas indicate that the best potential to infer soil moisture occurs during fall and spring. These periods encompass the growth stages

when soil moisture is most important to the winter wheat's yield. With further research, ESMR could be used to identify stress or drought conditions over winter wheat areas.

The results of this research indicate the general conditions which are necessary for the short wavelength ESMR to infer soil moisture. Atmospheric contributions, vegetation, and roughness produce detrimental effects to soil moisture detection at short microwave wavelengths. Longer wavelength radiometers such as the Scanning Multi-frequency Microwave Radiometer (SMMR) will lessen these dampening effects but resolutions will be larger. These longer wavelengths may be able to infer soil moisture over range, pasture, and densely vegetated croplands by using the same temporal mapping techniques that were used in this research.

6.0 LITERATURE CITED

Barnes, S. L. 1973: Mesoscale objective map analysis using weighted time-series observations. NOAA Tech. Memo., ERL NSSC-62, Norman, OK., 60pp.

Blanchard, B. J., M. J. McFarland, T. J. Schmugge, and E. Rhoades. 1979: Estimation of soil moisture with API algorithms and microwave emission. (Unpublished manuscript), 32pp.

Cihlar, J. and F. T. Ulaby. 1975: Microwave remote sensing of soil water content. Remote Sensing Lab. Tech. Rep. 264-6, University of Kansas Space Technology Center, Lawrence, KS., 183pp.

DeCoursey, D. G. 1974: Unpublished data.

McFarland, M. J. and B. J. Blanchard. 1977: Temporal correlations of antecedent precipitation with Nimbus 5 ESMR brightness temperatures. Preprints 2nd Conf. Hydrometeorology, Toronto, Ont., Canada, American Meteorology Society, Boston, MA., 311-315.

Meneely, J. M. 1977: Applications of the Electrically Scanning Microwave Radiometer (ESMR) to classification of the moisture content of the ground. Earth Satellite Corporation, Washington, DC., Final Report, 39pp.

Newton, R. W. 1977: Microwave remote sensing and its application to soil moisture detection. Tech. Rep. RSC-81, Remote Sensing Center, Texas A&M University, College Station, TX., 500pp.

Paris, J. F. 1971: Transfer of thermal microwaves in the atmosphere. NASA Grant NGR-44-001-098, Dept. of Meteorology Rep., Texas A&M University, College Station, TX. 257pp.

Saxton, K. E. and A. T. Lenz. 1967: Antecedent retention indexes predict soil moisture. J. Hydraul. Div., Proc. Am. Soc. Civ. Eng. Vol. 93, No. HY4, 223-241.

Schmugge, T. 1976: Preliminary results from the March 1975 soil moisture flight. Goddard Space Flight Center Rep. 913-76-216, Greenbelt, MD., 23pp.

1977: Remote sensing of surface soil moisture. Preprints, 2nd Conf. Hydrometeorology, October 25-27, 1977, Toronto, Ontario. American Meteorology Society, Boston, MA., 304-310.

Schmugge, T., P. Gloersen, T. Wilheit, and F. Geiger. 1974;
Remote sensing of soil moisture with microwave radiometer.
J. Geophys. Res. Vol. 79, No. 2, 317-323.

_____, B. J. Blanchard, W. J. Burke, J. F. Paris and
J. R. Wang. 1976a: Results of soil moisture flight
during April 1974. NASA Tech. Note TN D-8199, National
Aeronautics and Space Administration, Washington, DC.,
55pp.

_____, T. Wilheit, W. Webster, Jr. and P. Gloersen.
1976b: Remote sensing of soil moisture with microwave
radiometers-II. NASA Tech. Note TN-D-8321, National
Aeronautics and Space Administration, Washington, DC.,
34pp.

_____, J. M. Meneely, A. Rango, and R. Neff. 1977;
Satellite microwave observations of soil moisture vari-
ations. Water Resour. Bull., Vol. 13, No. 2, 265-281.

Theis, S. W. 1979: Surface soil moisture estimation with
the electrically scanning microwave radiometer (ESMR).
M.S. thesis, University Library, Texas A&M University,
College Station, 46pp.

A P P E N D I X A

A PAPER PRESENTED FOR PUBLICATION TO THE
AMERICAN WATER RESOURCES ASSOCIATION
WATER RESOURCES BULLETIN

ESTIMATION OF SOIL MOISTURE WITH API ALGORITHMS
AND MICROWAVE EMISSION

Bruce J. Blanchard, Marhsall J. McFarland,
Thomas J. Schmugge, and Edd Rhoades¹

ABSTRACT: Large area soil moisture estimations are required for global systems of crop yield estimation and flood prediction. Microwave sensor systems that as yet can only detect moisture at the surface have been suggested as a means of acquiring large area estimates. Measurements of soil moisture were studied to understand the correlation and inter-correlation between moisture in surface soil layers and moisture in deeper layers. Relations previously discovered between microwave emission at the 1.55 cm. wavelength and surface moisture as represented by an antecedent precipitation index were used to provide a pseudo infiltration estimation. Infiltration estimation based on surface wetness estimated on a daily basis were used to estimate soil moisture at a depth of 15 cm. by use of a modified antecedent precipitation index with good results ($R^2 = .7010$ and $R^2 = .7383$). The technique was modified and used to estimate soil moisture at 15 cm. depth when only an estimate of surface moisture each three days was available. Predictions based on estimation

¹Respectively, Remote Sensing Center, Texas A&M University, College Station, Texas 77843; NOAA Environmental Studies Service Center, College Station, Texas 77843; NASA/Goddard Laboratory for Atmospheric Sciences, Goddard Space Flight Center, Greenbelt, Maryland 20771; SEA-AR, Chickasha, Oklahoma.

of surface wetness at three day intervals resulted in R^2 value of .6811 and .7076 for the same date sets. The algorithms developed in this study can be used over relatively flat agricultural lands to provide improved estimates of soil moisture to a depth greater than the depth of penetration for the sensor.

INTRODUCTION

Large area soil moisture measurements are needed for two primary application areas. First to define the antecedent moisture condition of watershed surfaces prior to flood producing storms and secondly to provide objective numerical input to crop growth models.

To approach these needs we should understand that watershed runoff resulting from any one rainfall event is dependent on a complex interaction of several variables where one of the more significant variables is the moisture condition of the soil at the time the event begins. It can be readily understood that when the soil is saturated, the major portion of the rainfall will become runoff. Likewise, it can be reasoned that measurements of soil moisture can serve as an indicator of the amount of storage available in the soil profile for a portion of the rainfall falling on a watershed surface. Measurements of moisture conditions over large areas are at present difficult to obtain and therefore even crude estimates over watershed drainage areas may result in significant improvement of flood predictions. In the central plains area a measurement providing three or more levels of soil moisture (dry, medium, wet) pertaining to the top 20 cm. will likely be of significant value if it can be provided routinely each three days or less.

Soil moisture requirements for input to crop models on the other hand are required for depths of as much as 150 cm. and it is generally believed that they must be more accurate. Most experimental work concerned with soil moisture requirements of crops has been done on extremely small areas. Measurement of soil moisture in crop experiments has also been confined to discrete layers of soil with each layer being approximately 15 cm. in depth. The conventional practice has led to development of soil profile models using such depth increments. Little has been done to determine if the requirements for crop models can be relaxed to accommodate less detailed soil moisture data over large areas.

Large area estimates of moisture for both of these applications are conventionally derived from rainfall data collected at widespread locations. Such estimates are relatively good in areas with widespread low intensity rainfall. Unfortunately, the major food producing areas of the United States and watershed areas where flooding frequently occurs are subject to frontal convective storms. Such storms produce non uniform distribution of rainfall, and estimates based on the available rain gauge data are frequently poor. To compound the problem, the separation of rainfall into runoff and infiltration components is difficult on a large area. It would therefore seem more appropriate to estimate large area soil moisture directly.

Our ability to estimate soil moisture over large areas by conventional techniques is limited by three major problems. Spatial variability in physical characteristics of the soils, variation in crop canopies of agricultural lands and wide variations in local rainfall all tend to make

estimates based on point measurements prohibitive. In order to make such estimates on a regional or global basis it will be necessary to employ the use of spacecraft sensors that can integrate the soil moisture over an area. The verification that an appropriate sensor in space can indeed provide useful soil moisture measurements will require large scale measurement of ground information.

Recent attempts have been made to establish the capability of passive microwave sensors for estimating soil moisture in the surface soils by monitoring the microwave emission from the earth's surface. One passive microwave system, the Electrically Scanning Microwave Radiometer (ESMR), in particular, has provided data from space that has been correlated to an antecedent moisture index (API) by McFarland and Blanchard (1977). The relation between the sensor data and the API, illustrated in Figure 1, is valid only in non forested and relatively flat agricultural terrain.

At the present time, passive microwave systems on spacecraft employ wavelengths too short to effectively estimate soil moisture in the 0 to 22.8 cm. zone of the soil surface. The estimation of moisture in the surface zones by use of microwave systems is further complicated by the fact that penetration achieved is dynamic and is both wavelength and moisture dependent. Wavelengths of 21 cm. (1 band) have been shown by Newton (1977) to estimate moisture in the surface 20 cm. when soil moisture is low while only penetrating to approximately 5 cm. when the soil is wet. Other studies (Schmugge, 1974; Wilheit, 1978) have indicated that the sampling depth is only a few tenths of a

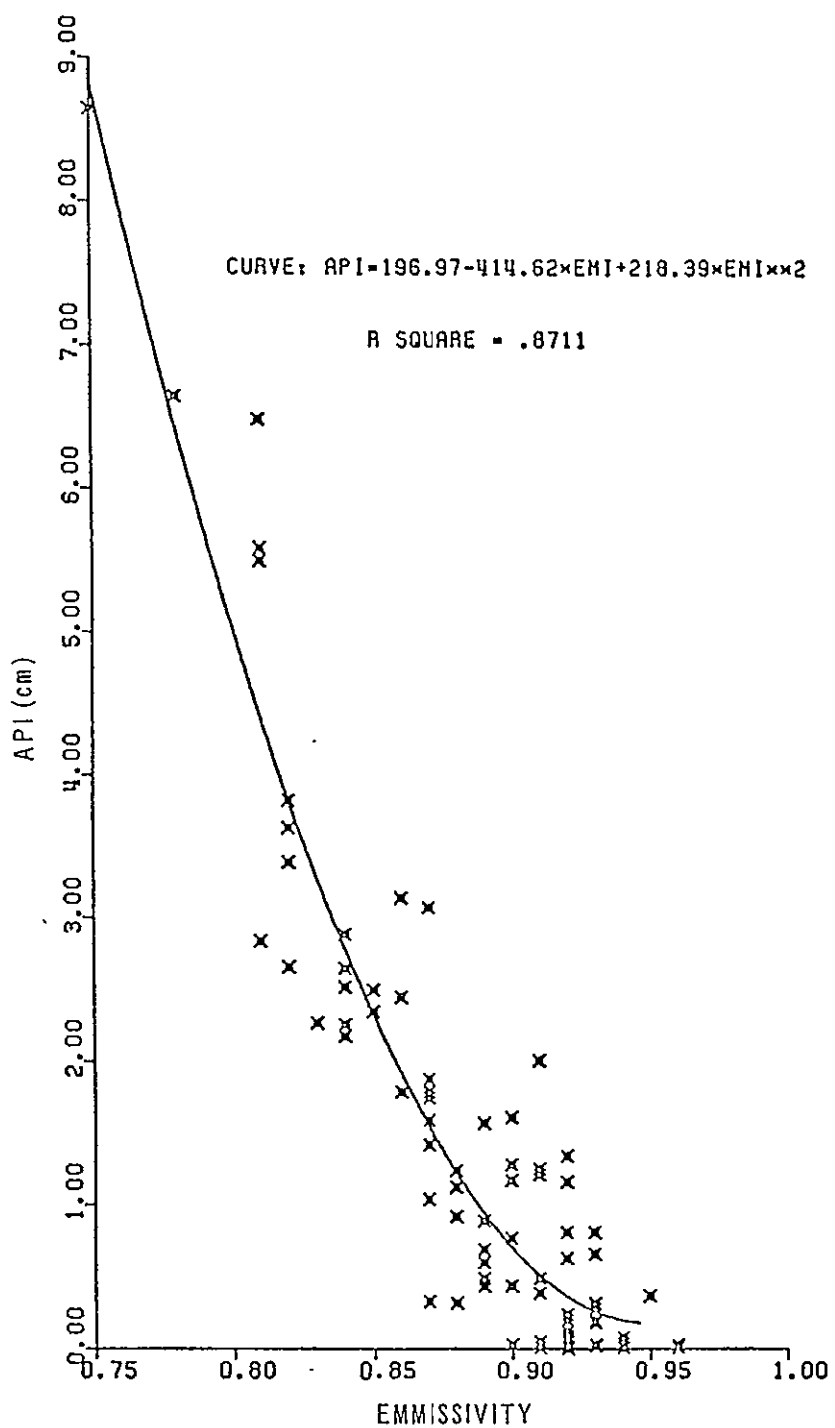


Figure 1. The relation between 1.55 cm microwave emission from the soil surface and an Antecedent Precipitation Index based on a time dependent depletion coefficient with a minimum value of .720. (From McFarland and Blanchard)

wavelength; i.e., 2.5 cm. at the 21 cm. wavelength. Wavelengths as long as one meter are currently being investigated and may provide an estimate of moisture in thicker surface zones more effectively than systems available now. Meanwhile, as an interim technique, an estimate of moisture in a significant depth of the surface soil might be derived from an algorithm using the antecedent precipitation index that represents the soil surface.

OBJECTIVE

The motivation for this study was the need to develop a technique where the ESMR or a similar microwave system can be used to produce a useful estimate of moisture in near surface soils. A better understanding of the relation between surface moisture and moisture in deeper layers of the surface, however, is necessary before we can extrapolate short wavelength microwave measurements of the surface to meaningful depths. The ESMR data are only related to an index of moisture at the surface since a wavelength of 1.55 cm. cannot achieve significant penetration in the surface. There may, however, be some means of relating these measurements to meaningful depths in the surface. This study was initiated to establish the relations between surface measurements by spaceborne passive microwave and estimates of soil moisture at some significant depth.

Related Studies

Numerous antecedent indices of moisture based on either rainfall or rainfall and runoff have been used by practicing hydrologists. Most

successful techniques are based on the fact that soil moisture depletion can be expressed as an exponential decaying function of the moisture input to the profile, Lindsey et al. (1949) and Chow et al. (1964), in the following form:

$$\text{API}_i = P_i + (\text{API}_{i-1})k_i \quad (1)$$

where: API = moisture index

P = daily effective rainfall or daily infiltration

k = depletion constant <1 and a function of time

i = day of the estimate

Several attempts have been made to improve on the basic concept by providing methods of estimating the depletion constant k. DeCoursey (Personal Communication) inverted a curve representing mean daily temperatures and found the general form of the curve represented the seasonal changes in k. Saxton (1967) investigated an extensive set of soil moisture data from two instrumented watersheds in Wisconsin and was able to establish that a seasonally variant k with a minimum value of .92 would provide a best estimate of moisture in the top 30 cm. A minimum value of .96 was most appropriate for soil moisture estimates in the top 91 cm. of soil; i.e., the decay of moisture in this layer is much slower. In Saxton's results, k values ranged up to .99 on April 1 and .98 on December 1. A curve representing his mean k values throughout the year is remarkably similar to the inverse of a curve through the mean monthly potential evapotranspiration (PET) calculated by the Penman equation. Saxton was able to predict best estimates of soil moisture as

a function of PET values by subtracting PET from moisture in the soil at times when the moisture available in the soil surface was above 60% of the field capacity. Computation for the latter approach requires the additional data for input to the Penman PET model.

Saxton also investigated the time required for calculations using Equation 1 to stabilize. The initial starting values have only short term effects when the time series begins with small values of the depletion constant k . The maximum time period that effects the initial input can be significant in less than 90 days.

Another approach to estimation of soil moisture has been taken in Russia by Basharinov et al. (1977). They reported attempts to extrapolate near surface soil moisture measurements to deeper depths with a technique based on the correlation between near surface soils and deeper layers for certain times of the year. In Basharinov's report, correlation between moisture in different zones are listed. Measurements for layers of soil less than 15 cm. from the surface were not in this study. In addition no mention was made of the time of day of the measurement. The high intercorrelations between shallow and deep surface zones implied that if the surface zone could be measured accurately, a reasonable estimate of moisture in a deeper zone could be made. No attempt was made to go one step further to relate the moisture measurements to antecedent rainfall. A review of these studies indicated that if the results of both Saxton and Basharinov could be verified, a technique might be developed to extrapolate surface measurements to a significant surface soil zone. This is the approach that will be tested here.

Data Used

Soil moisture estimates were available for sixteen unit source watershed drainage areas being studied by the Agricultural Research Service (ARS) at Chickasha, Oklahoma. Measurements with neutron probes had been collected over 75 months from four points within each area at time intervals of approximately fourteen days. The measurements were taken in a six hour time frame in mid day but no effort has been made to identify the diurnal fluctuation of the near surface measurement. This record encompasses a full range of soil moisture conditions.

The neutron measurements had been taken at depth intervals of 15.2 cm. beginning at that depth and continuing to 121.9 cm. Measurements for increments above the 15.2 cm. level were not available. The measurements were converted to estimated soil water in centimeters for each interval by using sensor calibration curves developed by SEA/AR. For this study, averages of the four points in each small drainage area are used.

Eight of the areas are devoted to native grasslands. Four of the grassland watersheds are located on silty soils derived from the Chickasha formation of the Permian red beds. Two of these have very poor vegetative cover while the other two have excellent native grass cover. The remaining four watersheds are located on sandy soils developed from Rush Springs sandstone and have a moderate cover of native grass.

Another eight drainage areas were located on cropland in the alluvial soils along the Washita River. These were devoted to cotton, wheat or alfalfa production. Crops were usually rotated on each area;

thus, the record does not represent any long period under a single crop. The period of record used began in June 1966 and extended to September 15, 1969; beginning again in January 1971 and ending on January 1, 1974. The last few months of the record covered the same time period used by McFarland and Blanchard in their study of correlations between ESMR data and API values. Also, the sampled areas are located within the area used in that study. These soil moisture records provide a data base that can be used to verify the correlations reported by Basharinov.

In addition, rainfall data were available for all of these drainage areas for the same period. The daily rainfall amounts were compiled for the four rangeland sites located on the Chickasha formation, R5, R6, R7 and R8 in order to study the relations between the antecedent precipitation index and the soil moisture of different surface zones.

ANALYSIS AND DISCUSSION

Simple correlation coefficients were calculated between soil moisture in the top 22.8 cm. and soil moisture in each incremental depth, Tables 1 and 2. Measurement of the moisture in this zone was made by a neutron probe reading at the 15.2 cm. depth. Correlation coefficients were also calculated between the soil moisture in the top layer and each depth of the surface zone, Tables 3 and 4. These latter correlations are representative of intercorrelated values since the surface 22.8 cm. are included in each surface zone.

Tables 1 through 4 confirm correlations reported by Basharinov and indicate that reasonable estimates of soil moisture at depths as great as

Table 1. Correlation between soil moisture in the top 22.8 cm. and soil moisture in other depth intervals within the profile on rangeland sites.

Depth Interval (cm.)	Depth Interval (in.)	Watershed Number								Combined Rangeland
		R1	R2	R3	R4	R5	R6	R7	R8	
0-22.8	0-9	1.0	1.0	1.0	1.0	1.0	1.0	1.0	1.0	1.0
22.8-38.1	9-15	.9137	.9195	.9134	.9222	.9269	.9172	.8741	.9455	.9184
38.1-53.3	15-21	.7169	.7676	.7802	.7841	.8411	.7978	.7265	.8786	.8437
53.3-68.6	21-27	.5373	.5924	.6265	.6409	.7661	.6915	.6031	.7885	.7655
68.6-83.8	27-33	.4615	.4484	.5178	.5231	.6448	.5705	.5465	.7077	.7060
83.8-99.1	33-39	.4106	.3467	.4160	.4121	.5340	.4656	.5547	.6763	.6779
99.1-114.3	39-45	.3614	.2579	.3360	.3311	.4726	.3967	.5828	.6429	.6566
114.3-129.5	45-51	.3497	.2149	.2697	.2280	.4524	.3527	.5338	.6629	.6264

Table 2. Correlation between soil moisture in the top 22.8 cm. and soil moisture in other depth intervals within the profile on cropland sites.

Depth Interval (cm.)	Depth Interval (in.)	Watershed Number								Combined Rangeland
		C1	C2	C3	C4	C5	C6	C7	C8	
0-22.8	0-9	1.0	1.0	1.0	1.0	1.0	1.0	1.0	1.0	1.0
22.8-38.1	9-15	.8461	.8862	.8788	.7585	.8771	.8543	.9081	.9137	.8795
38.1-53.3	15-21	.6722	.7291	.8034	.5456	.8136	.7824	.8258	.8265	.7794
53.3-68.6	21-27	.6009	.6042	.7785	.5078	.7545	.7261	.7356	.6611	.7276
68.6-83.8	27-33	.5529	.4690	.1879	.6499	.6500	.6034	.6963	.4924	.6483
83.8-99.1	33-39	.5586	.3941	.7426	.3882	.5020	.5239	.6179	.3710	.5945
99.1-114.3	39-45	.5150	.2986	.6715	.4348	.4637	.5000	.7319	.3195	.5055
114.3-129.5	45-51	.4545	.2160	.6670	.3886	.3268	.5061	.6299	.3290	.4170

Table 3. Correlation between soil moisture in the top 22.8 cm. and soil moisture in other surface intervals on rangeland sites.

Depth Interval (cm.)	Depth Interval (in.)	Watershed Number								Combined Rangeland
		R1	R2	R3	R4	R5	R6	R7	R8	
0-22.8	0-9	1.0	1.0	1.0	1.0	1.0	1.0	1.0	1.0	1.0
0-38.1	0-15	.9879	.9896	.9871	.9869	.9874	.9778	.9653	.9866	.9785
0-53.5	0-21	.9485	.9658	.9590	.9588	.9613	.9408	.9198	.9657	.9494
0-68.6	0-27	.8925	.9257	.9224	.9281	.9326	.9020	.8791	.9398	.9227
0-83.8	0-33	.8366	.8800	.8835	.8959	.9046	.8641	.8468	.9102	.8987
0-99.1	0-39	.7897	.8342	.8449	.8656	.8818	.8264	.8211	.8935	.8808
0-114.3	0-45	.7485	.7930	.8064	.8352	.8658	.7938	.8049	.8724	.8673
0-129.5	0-51	.7150	.7528	.7748	.8016	.8523	.7694	.7893	.8623	.8560

Table 4. Correlation between soil moisture in the top 22.8 cm. and soil moisture in other surface intervals on rangeland sites.

Depth Interval (cm.)	Depth Interval (in.)	Watershed Number								Combined Rangeland
		C1	C2	C3	C4	C5	C6	C7	C8	
0-22.8	0-9	1.0	1.0	1.0	1.0	1.0	1.0	1.0	1.0	1.0
0-38.1	0-15	.9628	.9802	.9662	.9503	.9699	.9679	.9772	.9803	.9675
0-53.3	0-21	.9060	.9453	.9312	.8688	.9382	.9305	.9456	.9564	.9227
0-68.6	0-27	.8586	.9129	.9078	.8073	.9115	.8989	.9136	.9332	.8881
0-83.8	0-33	.8262	.8840	.8540	.7591	.8846	.8627	.8991	.9109	.8583
0-99.1	0-39	.8085	.8433	.8746	.7131	.8541	.8243	.8851	.8928	.8376
0-114.3	0-45	.7972	.8011	.8611	.6863	.8291	.7926	.8756	.8778	.8159
0-129.5	0-51	.7829	.7575	.8511	.6614	.7922	.7701	.8656	.8630	.7914

50 or 60 cm. might be developed from measurement of a surface layer having sufficient thickness. An examination of the tables indicates that the rangeland areas produce higher correlations than the cropland measurements. There is also less variation in correlations between watershed areas than there is between the different cropland areas. This variation may be partially due to moisture extraction from variable root depths for the different crops as they are rotated year to year. There is also a possibility of supplemental non recorded watering by irrigation and the effects of tillage that are not reflected in the rainfall data.

Soil moisture and rainfall data from the four selected watershed areas R5, R6, R7 and R8 were used to investigate the effect of the coefficient k in Equation 1 on correlations between API and the soil moisture for different depths of the soil surface. The curve representing the seasonal change in k developed by DeCoursey, Figure 2, was compressed between selected minimum values and a constant January value of .994. Mean monthly values of k derived from the compressed curves were used to simplify the computations. Rainfall values used as input to the API equation were modified to account for the fact that a portion of the larger rainfall events ultimately becomes surface runoff. Storm rainfall minus recorded runoff was calculated for watersheds R5 and R7 and these values were plotted versus rainfall, Figure 3, to derive the relation between effective rainfall P_e and the recorded rainfall P , Figure 3, resulting in the following equation:

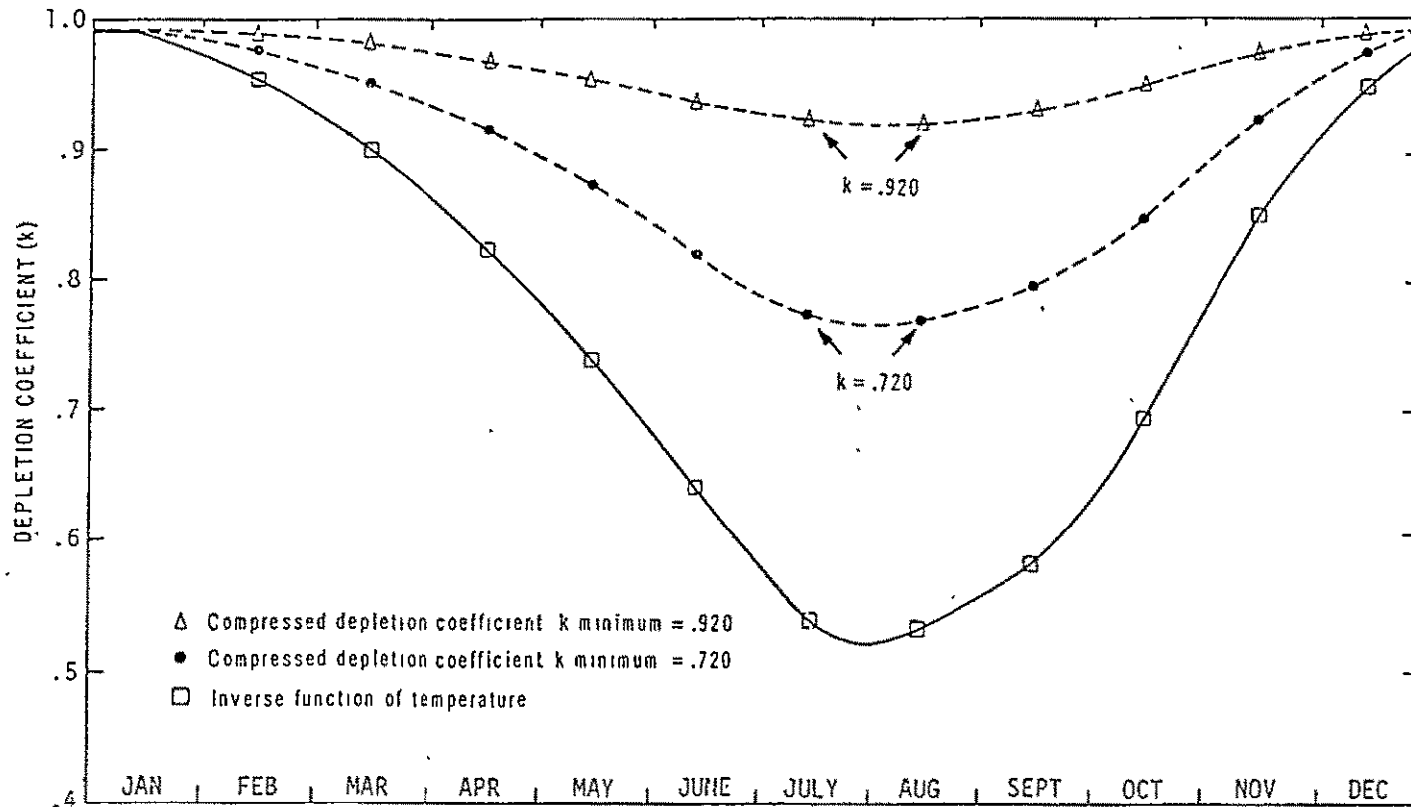


Figure 2. Typical depletion coefficients derived from an inverse temperature function (from DeCoursey) when related to different surface soil zones.

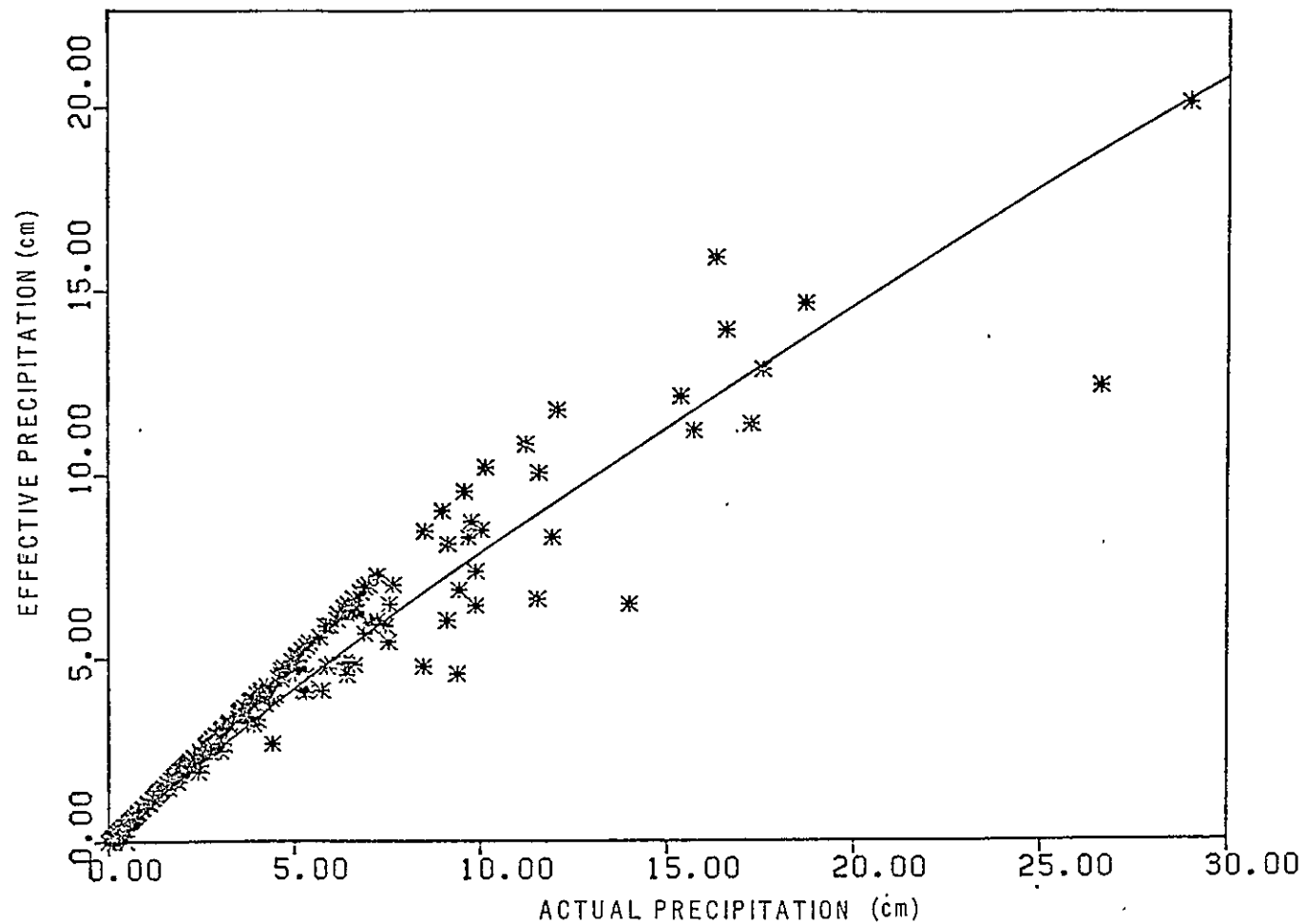


Figure 3. Least squares relation between actual precipitation and precipitation that did not run off the surface of watersheds R5 and R7.

$$P_e = P^{.829} \quad (2)$$

Combining equations 1 and 2 leads to the modified API equation used throughout this study.

$$API_i = P_{(i)}^{.829} + (API_{(i-1)})k_{(i)m} \quad (3)$$

where m - signifies the minimum monthly depletion constant.

Minimum values of k were varied from .84 to .98 by compressing the curves as shown in Figure 2 and simple correlations were then calculated between the API value and soil moisture in a discrete surface zone. Examples of the results are plotted in Figures 4 and 5 for two zones of the surface soils.

For the 0 to 22.8 depth interval, Figure 4, peak correlations were found when the minimum value of k was .92 for three of the four watershed areas. On watershed R6 the peak correlation occurred with a minimum k value of .90 with an R value of .7882 while the R value when k minimum was .92 is .7861, an insignificant difference. This surface zone can be best estimated with a minimum k value of .92.

When considering the correlation of API with a deeper surface zone, 0-83.3 cm., Figure 5, a larger minimum value of k is more appropriate. For this soil zone a minimum value of .94 is most effective. Generally in these calculations the correlations improve slightly with an increase in the minimum k value as the depth of the surface zone increases. Similar results were evident in Saxton's work.

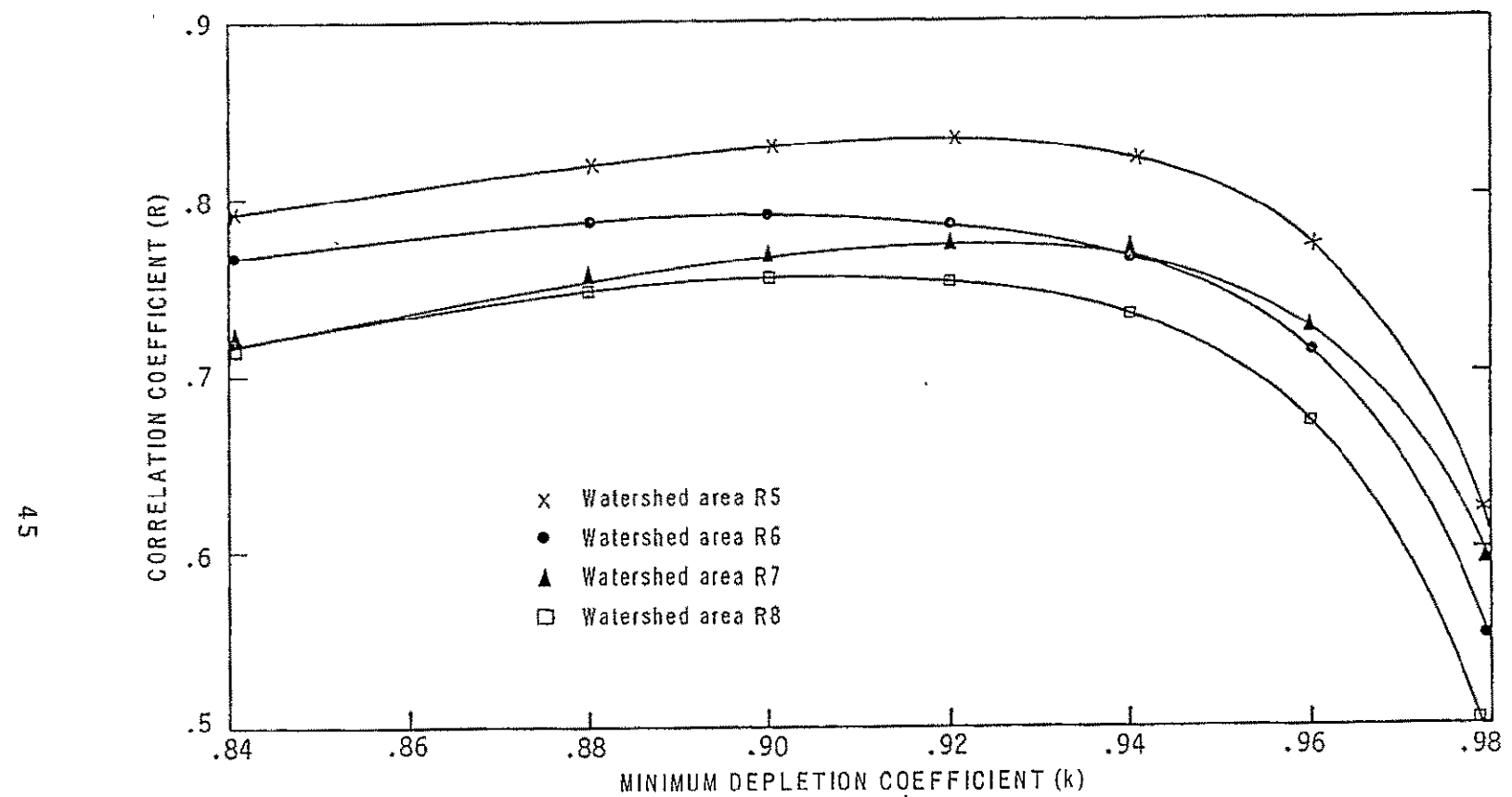


Figure 4. Changes in correlation between soil moisture in the surface 22.8 cm and the API values due to change in the value of the depletion coefficients.

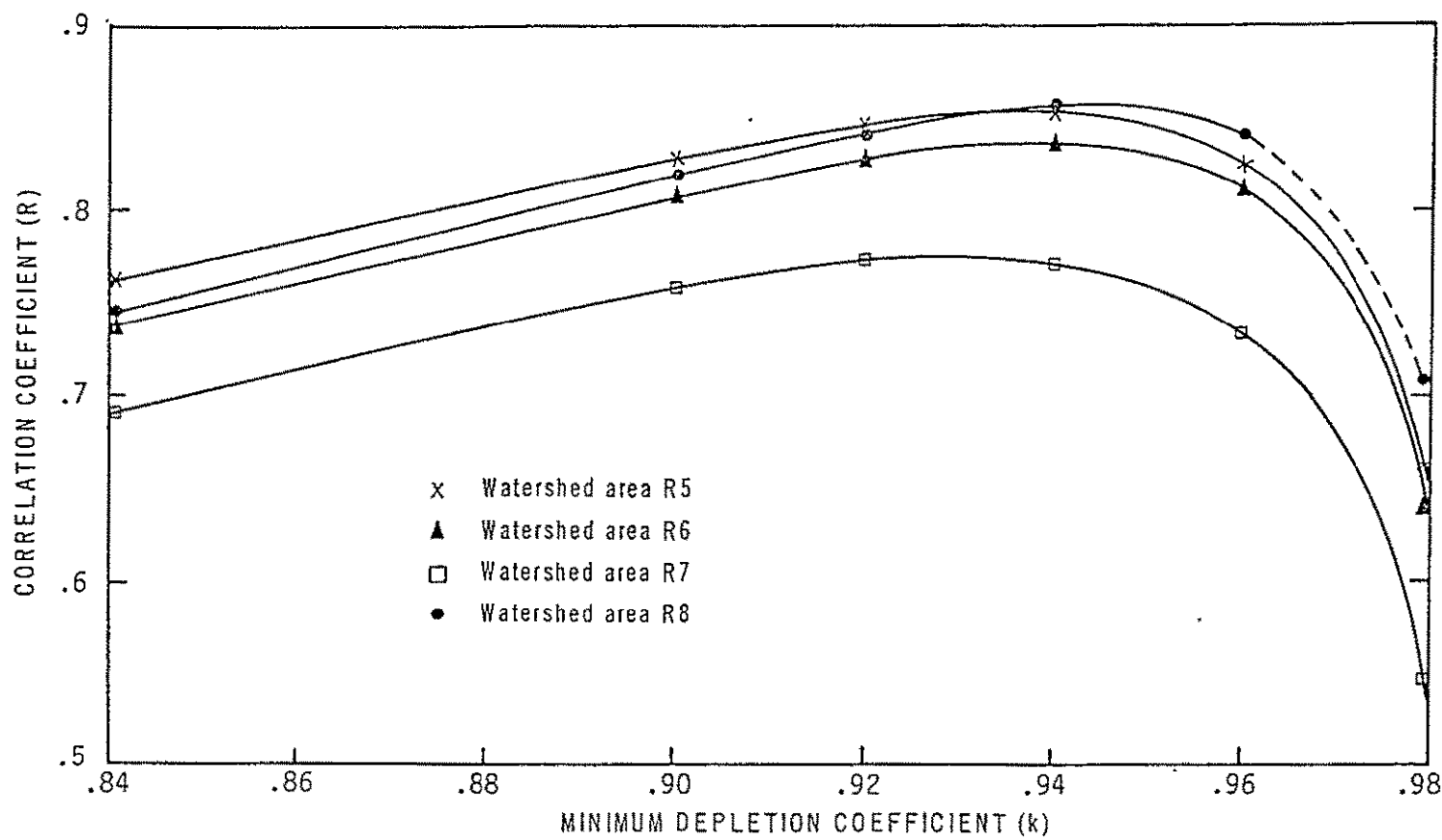


Figure 5. Changes in correlation between soil moisture in the surface 83.8 cm and the API values due to change in the value of the depletion coefficients.

McFarland and Blanchard found that the use of a very low .72 minimum k produced an API value that was best correlated to ESMR band (1.55 a wavelength) passive microwave sensor. Such a short wavelength provides no effective penetration into the soil volume and is therefore most sensitive to the wetness of the surface 1 or 2 cm. only. Soil moisture measurements were not available to investigate the 0 to 15 cm. depth increments of the near surface; however, it appears that optimum minimum values of k minimum change rapidly in the depths less than 20 cm. Using their data a second order equation can be developed to estimate API_{.72}

$$\text{API}_{.72} = 196.97 - 414.62\epsilon + 218.32\epsilon^2 \quad (4)$$

where ϵ = emissivity at 1.55 cm. wavelength coming from the soil surface.

Extrapolation of Surface Information to Estimate Soil Moisture

Surface wetness of the top 1 or 2 cm. if monitored frequently may serve as an indicator of rainfall distribution. When considered in this context, the measurement of the surface wetness might serve as a pseudo rainfall input to the API type estimator of soil moisture at a greater depth. Acceptance of this concept is imperative to the understanding of the following empirical development.

To proceed with this approach the available data for watersheds R5 and R7 were combined in a single set (R5&R7) to be used in the development of a prediction algorithm. Data from watersheds R6 and R8 were combined in a set (R6&R8) that was reserved for testing the algorithm.

Two series of daily API values were calculated for each set of data. One API value was based on a minimum k value of .92 and will be designated APIA and another series based on a minimum k value of .72 was designated APIB. APIB should be equal to API_{.72} in Equation 4 but has in this instance been calculated from rainfall.

The relation between actual soil moisture measurements (ASM) from the surface volume taken at 15 cm. depth and APIA values was first examined graphically. An equation was then fitted to the data by using an optimization technique described by DeCoursey and Snyder (1969). The technique resulted in an R^2 value of .7016 for the following equation:

$$ASM = 1.992 + .992 (\text{APIA})^{.610} \quad (5)$$

In order to use an equation of this form to predict soil moisture from remote sensing inputs, antecedent indicies must be developed that will simulate APIA. This requires some estimation of rainfall for input to Equation 1 that is a function of emissivity. APIB responds to rainfall in a similar fashion to the response of APIA to rainfall except that the decay of APIB is more rapid during summer months. By re-arranging Equation 1 it can be shown that the effective rainfall P^X can therefore be estimated by the following equation with the provision that P^X must be greater than or equal to zero.

$$P_i^X = \text{APIB}_i - (\text{APIB}_{i-1} \times k_{.72}) \quad (6)$$

Still using Equation 1, pseudo antecedent precipitation index (APIP) related to the surface 0-22.8 cm. but derived from the surface related

APIB can be calculated from the following equation:

$$\text{APIP}_i = [\text{APIB}_i - (\text{APIB}_{i-1} \times k_{(i)}(.72)] + \text{APIP}_{i-1} \times k_{(i)}(.92) \quad (7)$$

Substitution of Equation 7 into an equation of the form of Equation 5 produces a predicted soil moisture (PSM) as a function of APIB.

$$\text{PSM} = C_1 + C_2 [[\text{APIB}_i - (\text{APIB}_{i-1} \times k_{(i)}(.72) + [\text{APIP}_{i-1} \times k_{(i)}(.92)]].^{.61} \quad (8)$$

Coefficients cannot be optimized readily for this equation since APIP is a time series function of APIB. The coefficients were therefore found by first optimizing parts then adjusting the coefficients to produce a straight line fit between PSM and ASM with an intercept near zero and a slope near one. Coefficients C_1 and C_2 were found to be .024 and 1.431 respectively. The predictions resulting from this equation versus actual soil moisture content of the surface 0 to 22.8 cm. soil depth for the R5&7 data are shown in Figure 6. The prediction scheme was then tested on the R6&8 data resulting in the plot shown in Figure 7. R^2 values for the data in each plot were .7010 and .7387 for R5&7 and R6&8 respectively.

Now, it is doubtful if we can expect daily coverage from spacecraft systems in the immediate future. With present technology and funding a three day interval such as is provided by the ESMR sensor can reasonably be expected. The previous development of Equation 7 was based on daily measurement. To accommodate a three day coverage or availability of a measurement, modification of the equation is necessary.

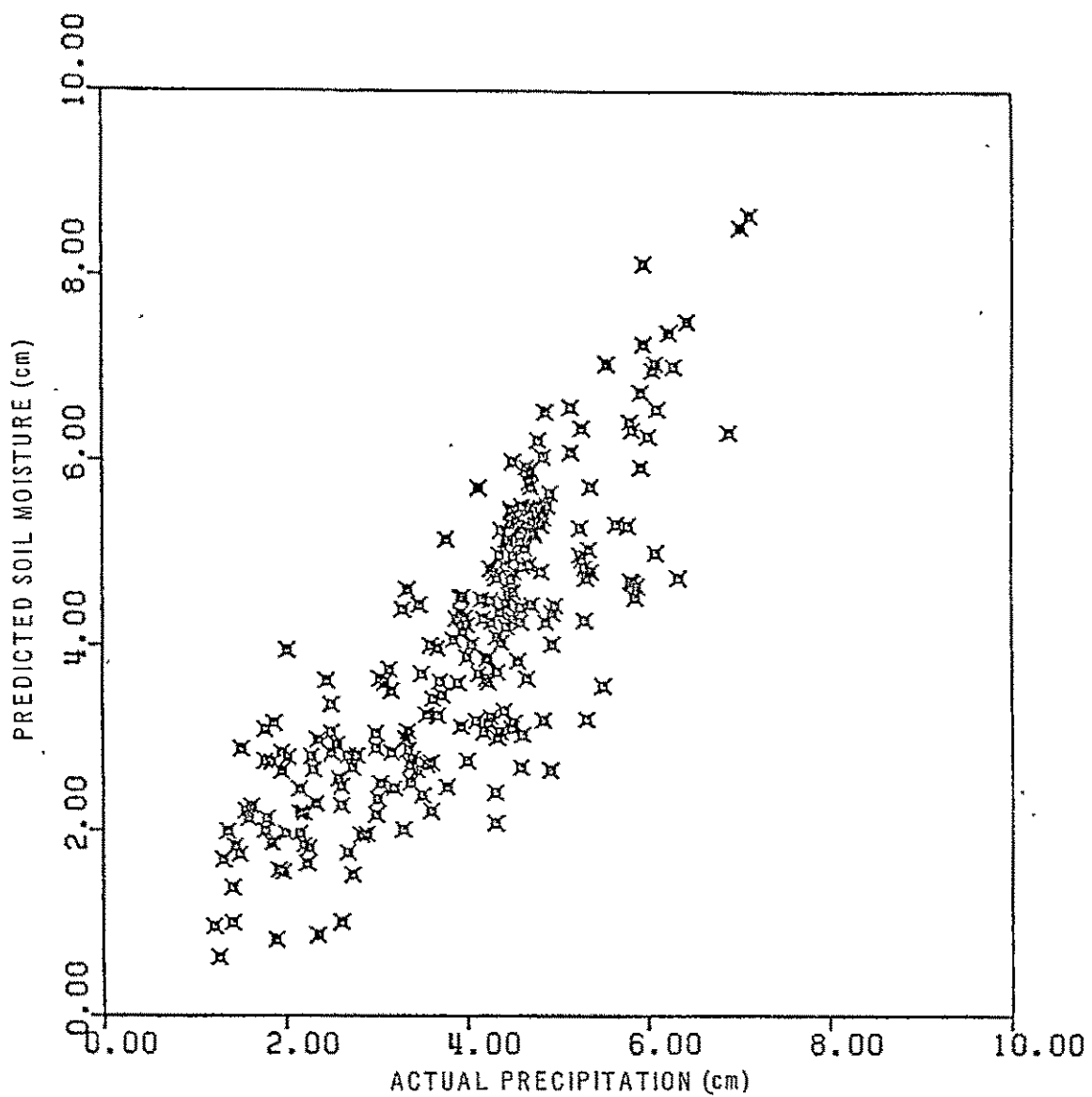


Figure 6. The relation between actual and predicted soil moisture in the top 22.8 cm. of soil on watersheds R5 and R7 where the algorithm was developed, $R^2 = .7010$. Predictions were based on daily calculations.

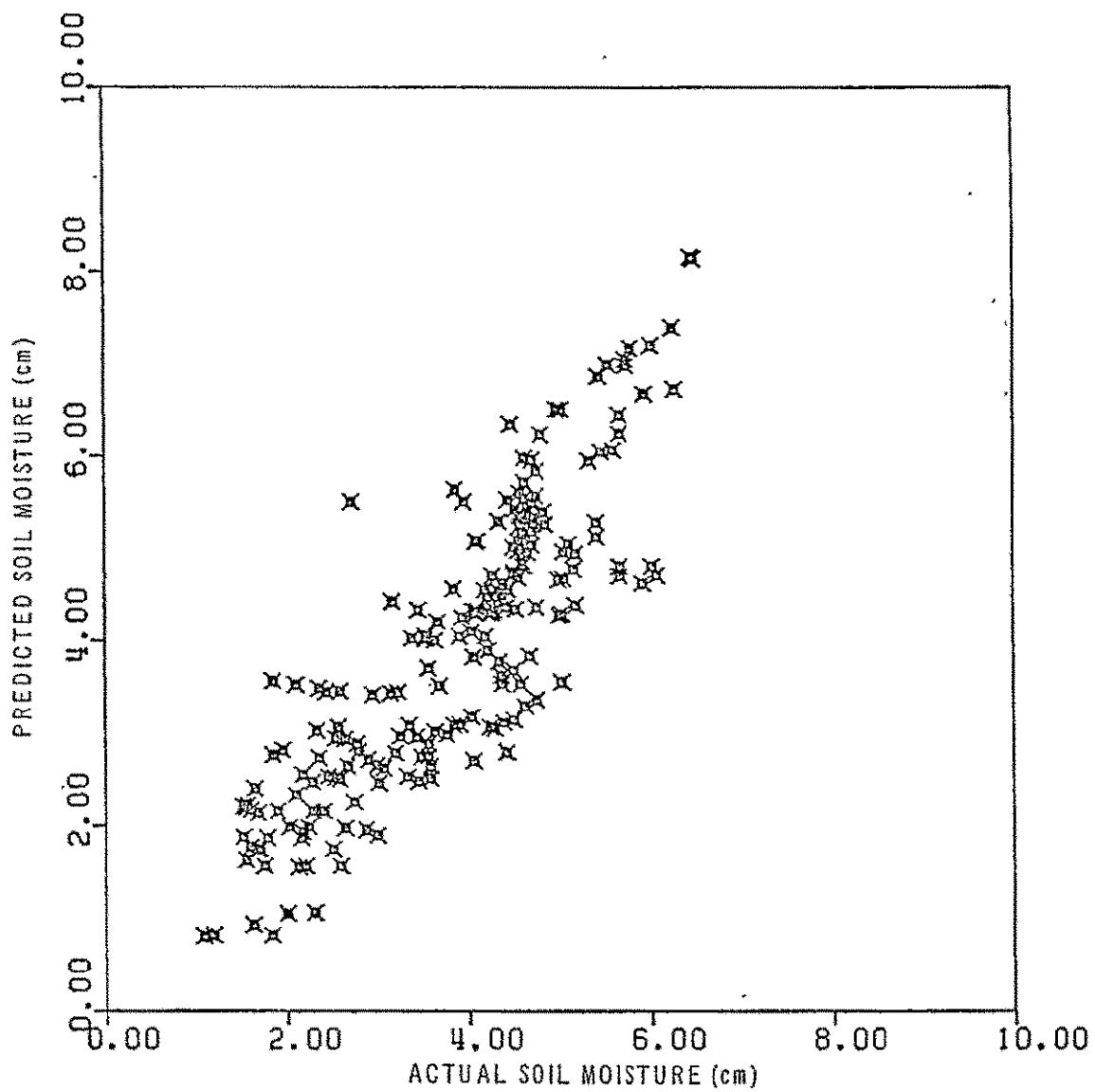


Figure 7. The relation between actual and predicted soil moisture in the top 22.8 cm. of soil on watersheds R6 and R8 where the algorithm was being tested, $R^2=.7387$. Predictions were based on daily calculations.

The change required is in the estimation of effective rainfall. Instead of depleting the APIB for the previous day by multiplication with the depletion coefficient (k), the APIB for day $(i-3)$ must be depleted for three days. The estimator of the effective precipitation then becomes

$$P^X = [APIB_{(i)} - (APIB_{(i-3)} \times k_i^3)] \quad (9)$$

The data for R5&7 were again used to establish the coefficients for an equation representing predicted soil moisture as a function of APIB. The resulting equation for prediction of soil moisture based on availability of an estimate of APIB each three days follows. A noticeable change in the second coefficient in the equation is necessary to adjust the slope of the predicted soil moisture values.

$$PSM = .12 + .765 [[APIB_i - APIB_{(i-3)} \times k_{(i)}^3 (.72) + \\ [APIB_{i-1} \times k_{(i)} (.92)]]^{.610}] \quad (10)$$

Predicted soil moisture resulting from use of equation 9 was correlated with R5&7 and R6&8 resulting in R^2 values of .6811 and .7076 respectively, Figures 7 and 8. The prediction capability then using the data available from observations each three days are not significantly different than they would be with daily observations. Similar equations could be developed to accommodate other repeat cycles of remote sensor data and thus produce a predicted soil moisture at two day or four day intervals.

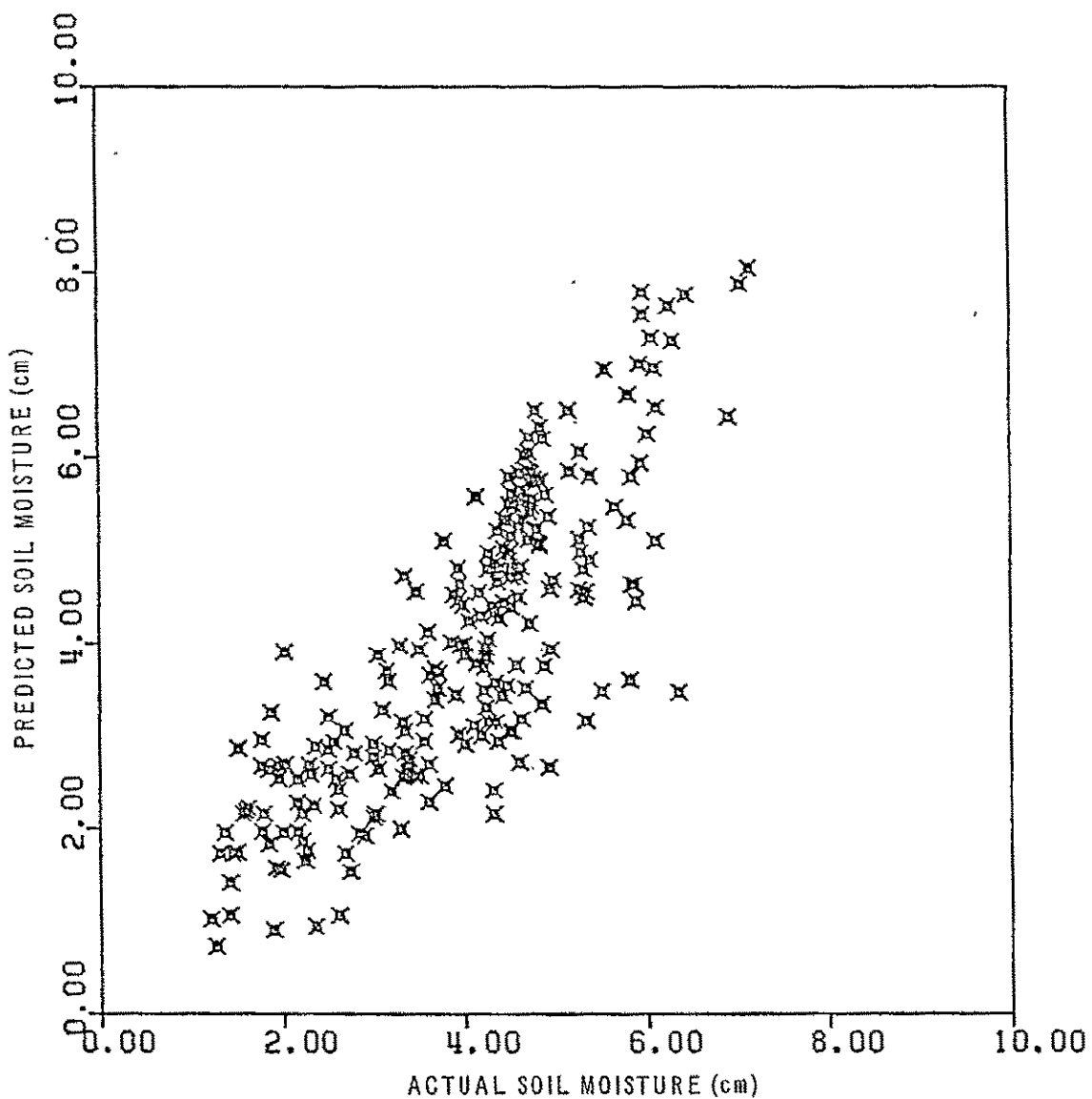


Figure 8. The relation between actual and predicted soil moisture in the top 22.8 cm. of soil on water-sheds R5 and R7 where the algorithm was developed, $R^2 = .6811$. These predictions were based on the assumption that measurements of the surface would only be available each third day during the year.

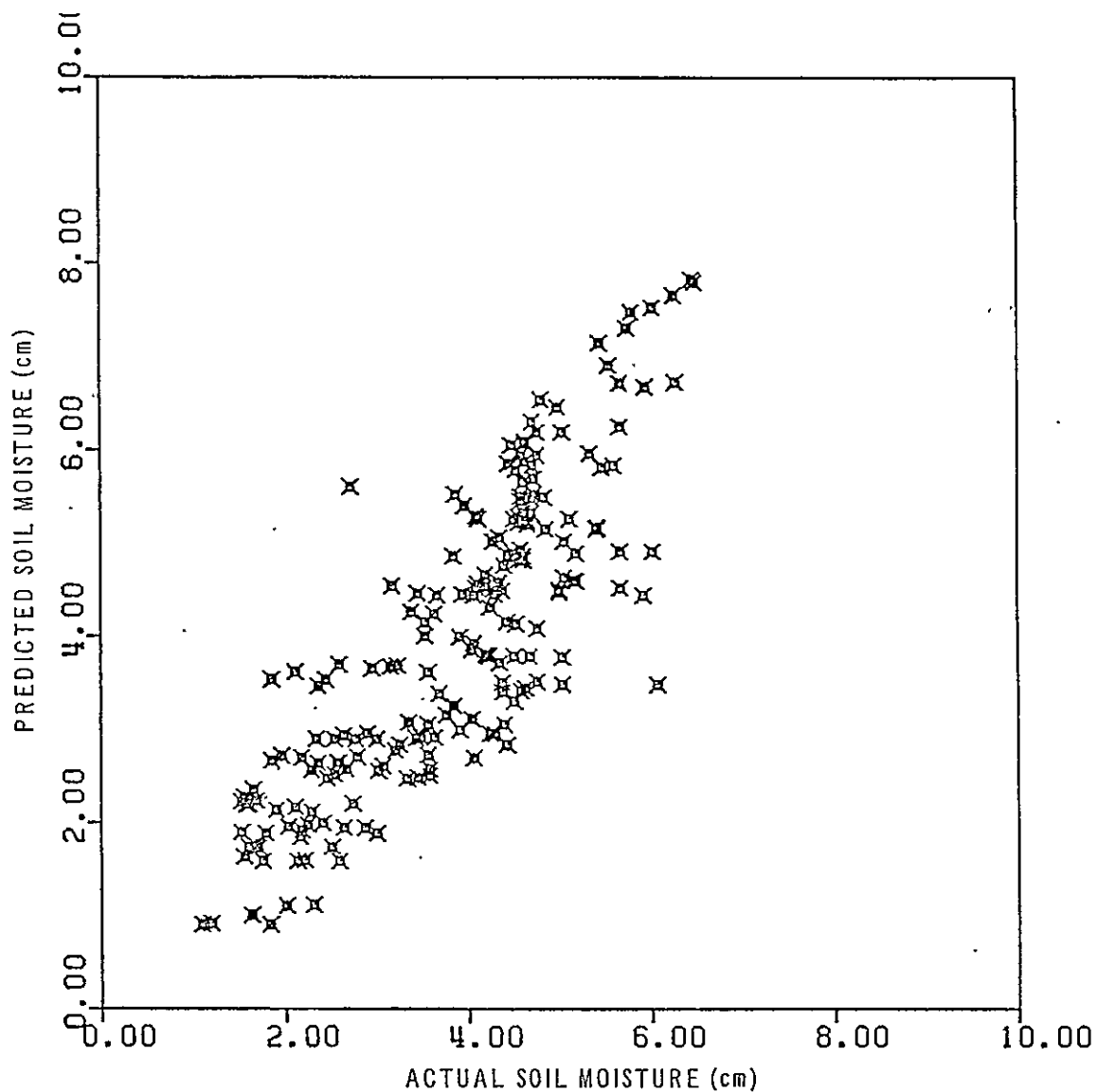


Figure 9. The relation between actual and predicted soil moisture in the top 22.8 cm. of soil on watersheds R6 and R8 where the algorithm was being tested, $R^2 = .7076$. These predictions were based on the assumption that measurements of the surface would only be available each third day during the year.

OBSERVATIONS AND DISCUSSION

The development of the preceding algorithms for estimation of soil moisture are based on coefficients suitable for a surface layer approximately 22.8 cm. thick. It is obvious that thicker surface layers can be estimated by increasing the minimum coefficient used to calculate APIP. Examination of Tables 1 through 4 indicate that correlations between predicted and actual soil moisture would rapidly decay with added depth beyond about 80 cm. Some of the root zone measurements requested by agricultural users therefore may not be reliable when using this technique.

The technique can be applied in limited areas with the existing K band (1.55 cm. wavelength) system already in global operation. Good estimation of surface wetness with ESMR data is restricted to areas where large relatively flat surfaces are observed. Rough terrain has significant influence on the sensor return and in those areas this technique may not work well with the ESMR data. Added benefits could be obtained with a longer wavelength and a slightly better resolution than is currently available. It would seem advisable to use existing and near future passive microwave sensors to provide the estimates while long range experiments are conducted to determine optimum systems.

Flood prediction applications in regions where forests and extreme roughness are not prevalent can definitely benefit from this technique. Agricultural applications, especially the crop yield estimation for small grains, could readily use this technique in the next decade when

more sophisticated sensors will be unavailable on a regular basis.

In the course of this study the data used from the Southern Great Plains Watershed Research Center and other sets of data available were examined. In the search for data to accomplish this study it became apparent that there is a totally inadequate supply of long term soil moisture data that is applicable to areas larger than a few square meters. Problems in measurement, calibration, manpower and funding indicate that large scale ground sampling under spaceborne systems is impractical, if not physically impossible. It is likely therefore that indicies such as the API may be the best measure available for testing of space borne sensors.

CONCLUSIONS

This study has resulted in the following conclusions:

1. Correlations and intercorrelations between near surface soil moisture and deeper layers have been shown. These correlations are comparable to those reported in Russia by Basharinov et al.
2. Algorithms for prediction of soil moisture in the surface 22.8 cm. of soil have been defined and tested on independent data sets.
3. The above algorithms can readily be used to input remote sensing data from a passive microwave imager to an equation that will estimate soil moisture at a depth greater than the system can sense.
4. An interim system for estimation of soil moisture in relatively smooth terrain for use in flood prediction and crop yield estimates for small grains should be feasible when the algorithms in this report are applied.

5. More universal application of the algorithms defined can be possible when passive microwave sensors with wavelengths long enough to penetrate more dense vegetation become available in space.

LITERATURE CITED

Basharinov, A. Ye, B. M. Liberman, Peutov, Ye. A., A. A. Chukhlantsev and A. N. Shutko. 1977. Results of U.H.F. Ratiometric and Direct Ground Measurement of Soil Moisture in 1976, Report of Soviet and American Working Group. NASA TT Technical Translation F-17521.

Chow, Ven T., et al. 1964. Handbook of Applied Hydrology. McGraw-Hill Book Company, Inc., New York. Section 21, Hydrology of Agricultural Lands, pp. 21-1 to 21-05 by Ogrosky, H. O., and Mockus, V. 1964.

DeCoursey, Donn G. and Willard M. Snyder. 1969. Computer-Oriented Method of Optimizing Hydrologic Model Parameters. *Journal of Hydrology* 9; 34-36.

Lindsey, Ray K., Jr., Max A. Kohler and Joseph L. Paulhus. 1949. Applied Hydrology. McGraw-Hill Book Company, Inc., New York.

McFarland, Marshall J. and Bruce J. Blanchard. 1977. Temporal Correlations of Antecedent Precipitation with Nimbus 5 ESMR Brightness Temperatures. Second Conference on Hydrometeorology, Toronto, Ontario, Canada.

Newton, Richard Wayne. 1977. Microwave Remote Sensing and Its Application to Soil Moisture Detection. Technical Report RSC-81, Remote Sensing Center, Texas A&M University, College Station, Texas.

Saxton, Keith E. and Arno T. Lenz. 1967. Antecedent Retention Indexes Predict Soil Moisture. *Journal of the Hydraulics Division, Proceedings of the American Society of Civil Engineers*.

Schmugge, T., P. Gloersen, T. Whilheit and F. Geiger. 1974. Remote Sensing of Soil Moisture with Microwave Radiometers. *Journal of Geophysical Research*. 79(2).

LITERATURE CITED (continued)

Wilheit, T. 1978. Radiative Transfer in a Plane Stratified Dielectric.
IEEE Trans. Geosci. Elec., GE-16, 138-143.

A P P E N D I X B

ABSTRACT OF PAPER PRESENTED AT
1979 SPRING AGU MEETING

CORRELATIONS OF BRIGHTNESS TEMPERATURES FROM THE ELECTRICALLY SCANNING MICROWAVE RADIOMETER (ESMR) WITH ANTECEDENT PRECIPITATION INDICES (API)

M. J. McFarland (Dept. of Agricultural Engineering,
Texas A&M University, College Station, Tx.)

B. J. Blanchard, S. W. Theis (Remote Sensing Center,
Texas A&M University, College Station, Tx.)

Estimates of soil moisture in a large area context are primarily useful for large area crop monitoring and for estimation flood hazards on large and small drainage areas. Such estimates may also provide indications of soil moisture below the surface as well as provide a means for the determination of drought and areal extent of drought conditions. A preliminary study correlated digital data from the ESMR to API that in turn is correlated to soil moisture over the northwestern third of Oklahoma. Encouraging results were obtained for a three month period in the fall of 1973 when vegetation was sparse. Since the ESMR is a quasi-operational system, data can be acquired over the same area on a three day repeat cycle. This provides the opportunity to investigate changes in soil moisture through a time series. Temporal mapping reduces the effects of the point to point variations in vegetative cover, surface roughness, and soil characteristics.

The moisture content and temperature of the emitting layer integrated over the sensor footprint forms the major variations of the temporal brightness temperature changes. Since the emitting layer temperature can be approximated, the brightness temperature changes may provide a fairly accurate indication of soil moisture changes for rainfall and subsequent drying.

The REMOTE SENSING CENTER was established by authority of the Board of Directors of the Texas A&M University System on February 27, 1968. The CENTER is a consortium of four colleges of the University; Agriculture, Engineering, Geosciences, and Science. This unique organization concentrates on the development and utilization of remote sensing techniques and technology for a broad range of applications to the betterment of mankind.

